6-1-1979

The Modification of Simple Images by Fourier Transform Manipulation

Noel Chavez

THE MODIFICATION OF SIMPLE IMAGES BY FOURIER TRANSFORM MANIPULATION

by

Noel Chavez

A thesis submitted in partial fulfillment
of the requirements for the degree of
Bachelor of Science in the School of
Photographic Arts and Sciences in the
College of Graphic Arts and Photography
of the Rochester Institute of Technology

June, 1979

Signature of the Author.....
Photographic Science
and Instrumentation

Certified by.....
Thesis Adviser

G-925588

Abstract

Knowledge of how an image is changed by a given modification of its Fourier transform is important when attempting to find solutions to problems in image processing. Several types of filters were used to modify the Fourier transforms of an edge and a bartarget. The images were reconstructed from the modified transforms to determine the change produced by a given modification. Various regions of the Fourier transform determine specific characteristics of the image. The amplitude of the low frequencies controls the form and average level of the image, while the amplitude of the high frequencies effects sharp transitions and noise.

TABLE OF CONTENTS

INTRODUCTION

Any object which can be represented by a function in the spatial domain can also be represented by a corresponding function in the frequency domain. The frequency domain representation of the object defines the frequency and amplitude of the various sinusoids of which it is composed. The two representations of the object are related through the Fourier transform. By computing the Fourier transform of the object in the spatial domain, the object is separated into its sinusoidal components. The spatial domain representation of the object can be reconstructed from its sinusoidal components by computation of the inverse Fourier transform.

When the relative amplitude of various frequencies of the Fourier transform of the object are changed, the object is modified upon reconstruction. The object is changed, because the Fourier transform from which it is being reconstructed has been modified. Various modifications in the Fourier transform of an object produce different modifications in the object when reconstructed. Many problems in image processing can be solved using this and other properties of the Fourier transform.

INTRODUCTION, continued

The purpose of this work is to modify simple images utilizing the properties of the Fourier transform, to determine the character and magnitude of its Fourier transform and to become familiar with various aspects and techniques of digital image processing.

Theory

A great number of problems in image processing require the application and make use of the unique properties of the Fourier transform. Most available mathematical treatments of the Fourier transform deal with continuous functions.[1] However, in most if not all cases involving the detection and recording of a signal, information is collected and stored as discrete data. That is, a continuous signal is specified by physical measurements made at regular intervals of time or space.[2] Since very few processes or events can be accurately or even approximately specified by exact mathematical relationships, discrete data must be used. If a function is represented by a series of values taken at discrete intervals, its Fourier transform cannot be computed by normal continuous methods. An alternative means is required. The discrete Fourier transform is a special case of the continuous Fourier transform, and is the only means whereby the Fourier transform can be computed from discrete data. With the capability of today's computers to store and process large quantities of data the use and application of the discrete Fourier transform in image processing is fast and efficient.

A good way to understand the discrete Fourier transform is to start with a continuous function and its

Fourier transform, and modify them so that they are in a form which a computer may store and process them.[3] Let a continuous function be represented by h(x) and its Fourier transform by H(f), where f is specified as some frequency in cycles/mm.

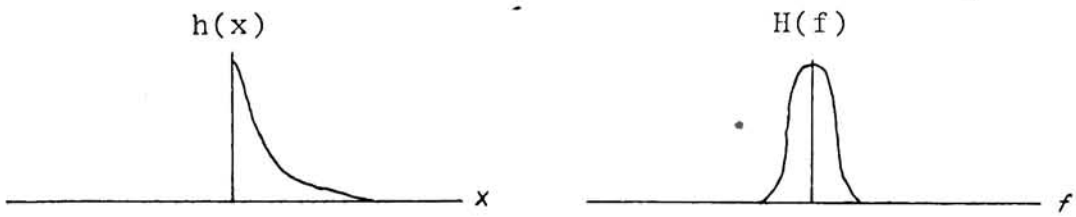

Figure 1

Since computers are only capable of storing discrete data, the function h(x) must be sampled. Sampling is accomplished by multiplying h(x) by a series of delta functions separated by a distance Δx.[4] If s(x) is the sampling function, then

$$s(x) = \sum_{k=-\infty}^{\infty} \delta(x - k\Delta x) \qquad \text{Equation 1}$$

The Fourier transform of the sampling function is S(f), which is also a series of delta functions, this time separated by a distance $1/\Delta x$ in the frequency domain,

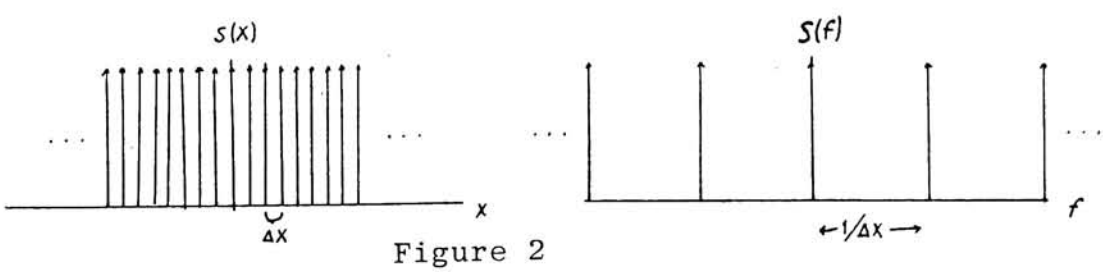

Figure 2

The sampled function is specified as

$$h(x)s(x) = h(x)\sum_{k=-\infty}^{\infty} \delta(x - k\Delta x). \qquad \text{Equation 2}$$

By definition

$$f(x)\,\delta(x - x_0) = f(x_0)\,\delta(x - x_0), \qquad \text{Equation 3}$$

then

$$h(x)\,s(x) = \sum_{k=-\infty}^{\infty} h(k\Delta x)\,\delta(x - k\Delta x). \qquad \text{Equation 4}$$

The sampled function is now a series of delta functions of varying amplitude.[5] In the frequency domain something quite different takes place. By the convolution theorem we know that the Fourier transform of the product of two functions is the convolution of their Fourier transforms. In this case

$$\mathcal{F}[h(x)s(x)] = H(f) * S(f) \qquad \text{Equation 5}$$

Since S(f) is a series of delta functions, the result of the convolution of H(f) with S(f) is to make H(f) a periodic function with a period of $1/\Delta x$

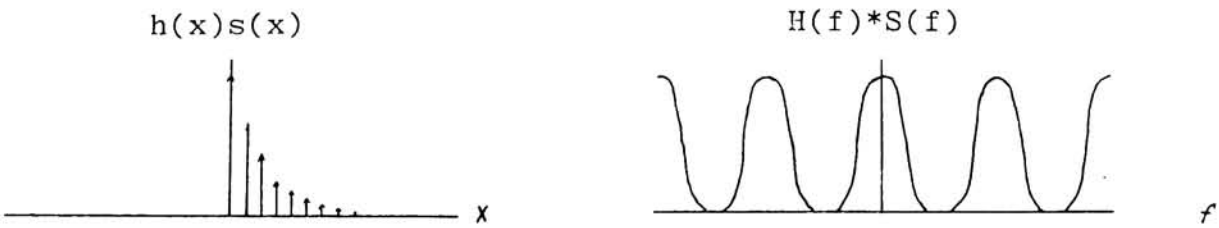

Figure 3

It is of course impossible to take an infinite number of samples, therefore sampling must occur over a finite interval. The sampled function h(x)s(x) must be truncated. Truncation is accomplished by multiplying the sampled functions by a rectangular function. Let the truncating function be t(x) where

$$t(x) = \begin{cases} 1 & |x| \leq X_o/2 \\ 0 & |x| > X_o/2 \end{cases} \qquad \text{Equation 6}$$

The Fourier transform of the truncating function is T(f) where T(f) is a sinc function whose first zero occurs at $1/X_o$.

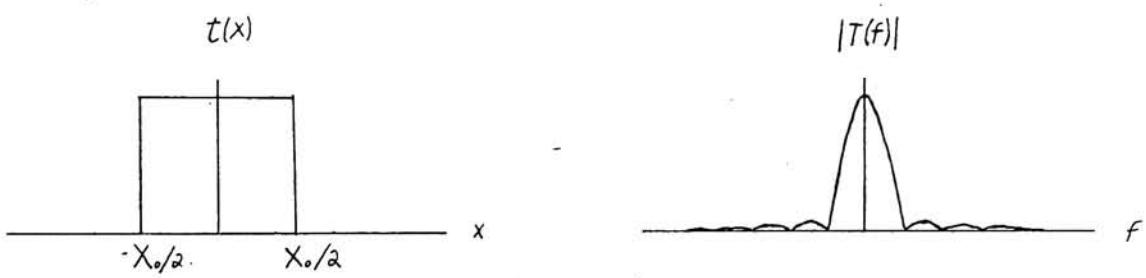

Figure 4

The truncated sampled function is the product of the simplified function and the truncating function and is specified as

$$h(x)s(x)t(x) = \left[\sum_{k=-\infty}^{\infty} h(k\Delta x)\delta(x - k\Delta x)\right] t(x) \qquad \text{Equation 7}$$

If there are N sample intervals within the truncation interval, then the limits of the summation become finite and

$$h(x)s(x)t(x)= \sum_{k=0}^{N-1} h(k\Delta x)\delta(x-k\Delta x) \qquad \text{Equation 8}$$

Because the truncated sampled function is the product of the sampled function and the truncating function, the Fourier transform of the sampled function is convolved with T(f) so that

$$F[h(x)s(x)t(x)]= [H(f)*S(f)] *T(f) \qquad \text{Equation 9}$$

The result of Equation 9 is to produce "ringing" in the Fourier transform of the truncated sampled function

h(x)s(x)t(x) [H(f)*S(f)]*T(f)

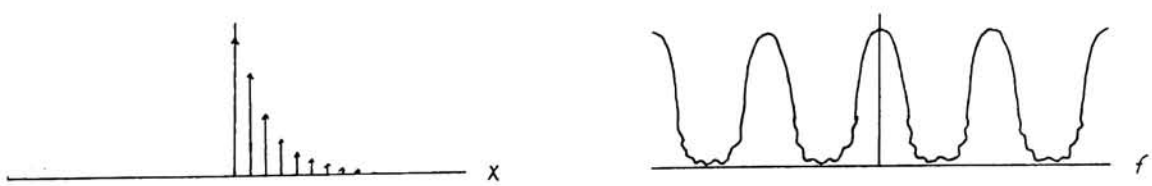

Figure 5

The "ringing" or rippling is due to the fact that the convolution in Equation 9 involves a sinc function.

The side-lobes of the sinc function create "ringing" in the resulting function. "Ringing" is an inherent error produced by the computation of the discrete Fourier transform. To minimize the error due to "ringing", it is important to use a truncation interval as wide as possible. The reason for this lies in the fact that as the width of the rectangle function used to truncate the function increases, the width of the rectangle function used to truncate the function increases, the width of its Fourier transform, the sinc function, decreases and more closely approximates an impulse function.[7]

One final operation is required to make the Fourier transform pair suitable for processing by computer. From Figure 5, it can be seen that the original function is now represented by a finite series of delta functions of varying amplitude. The Fourier transform of the function however, is a continuous periodic function. The transform must now be sampled so that it also is represented by a series of discrete values. Again, sampling is performed by multiplying the transform by a series of delta functions. The sampling function is specified as $\Delta(f)$. The tranform of the sampling function is $\Delta(x)$ which is defined as

$$\Delta(x) = X_0 \sum_{r=-\infty}^{\infty} \delta(x - rX_0) \qquad \text{Equation 10}$$

where X_o is the separation of the delta functions in the spatial domain.

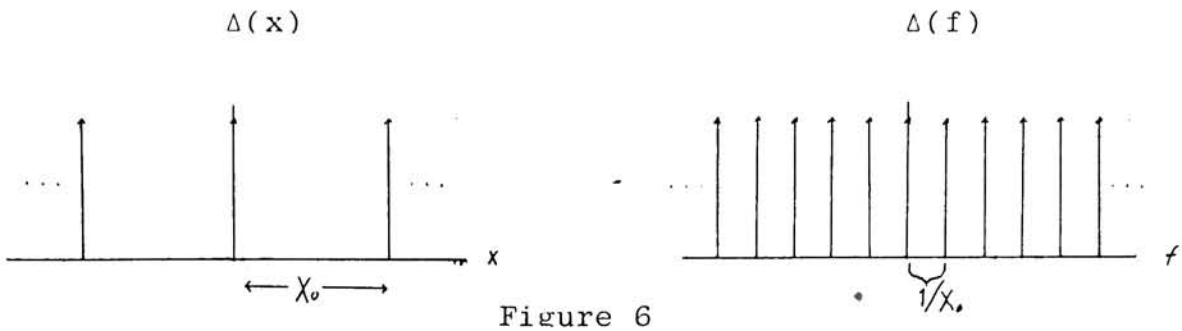

Figure 6

Since the transform is being multiplied by the sampling function Δ(f), then the sampled truncated function must be convolved with Δ(x).[8] That is.

$$[h(x)s(x)t(x)]*\Delta(x) = \left[\sum_{k=0}^{N-1} h(k\Delta x)\delta(x-k\Delta x)\right]*\left[X_o\sum_{r=-\infty}^{\infty}\delta(x-rX_o)\right],$$

Equation 11

which reduces to,

$$X_o\sum_{r=-\infty}^{\infty}\left[\sum_{k=0}^{N-1} h(k\Delta x)\delta(x-k\Delta x-rX_o)\right].$$

Equation 12

As a result of this convolution, the sampled truncated function becomes periodic as shown by Figure 7.

[h(x)s(x)t(x)]*Δ(x) [H(f)*S(f)]*|T(f)|]Δ(f)

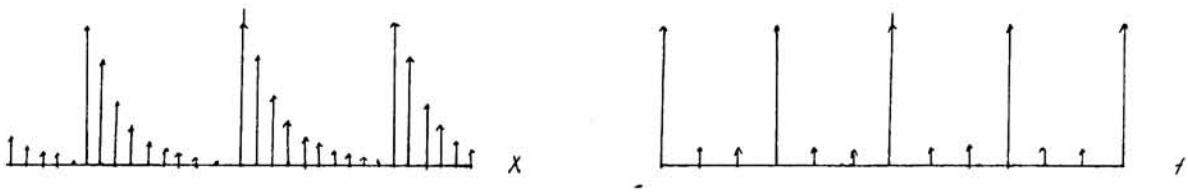

Figure 7

The Fourier transform pair is now in a form where both are represented by a series of a discrete values, and both are periodic functions.

The sampled function is periodic and is specified by

$$h^1(x) = X_0 \sum_{r=-\infty}^{\infty} \left[\sum_{k=0}^{N-1} h(k\Delta x)\, \delta(x - k\Delta x - r X_0) \right]. \qquad \text{Equation 13}$$

By definition the Fourier transform of a periodic function is

$$F(f) = \sum_{n=-\infty}^{\infty} C_n\, \delta(f - n f_0), \qquad \text{Equation 14}$$

which is a sequence of equidistant delta functions of varying magnitude.[9] Notice that the Fourier transform of a periodic function is not continuous. Cn represents the Fourier coefficients of the function. In this case the Fourier transform of $h^1(x)$ is

$$H^1\left(\frac{n}{X_0}\right) = \sum_{n=-\infty}^{\infty} C_n\, \delta(f - n f_0), \qquad \text{Equation 15}$$

where f_o is the distance between the frequencies where the function exists and

$$f_o = 1/X_o. \qquad \text{Equation 16}$$

As stated earlier there are N number of samples in the interval X_0, and each sample is separated from the adjoining samples by a distance Δx, therefore

$$X_o = N\Delta x \quad \text{and} \quad f_o = 1/N\Delta x. \qquad \text{Equation 17 \& Equation 18}$$

Cn is the Fourier coefficients of the function and is defined as

$$C_n = \frac{1}{X_o}\int_{-\Delta X/2}^{X_o-\Delta X/2} h^1(x)\, e^{-i2\pi nX/X_o}\, dx. \qquad \text{Equation 19}$$

Substituting for $h^1(x)$

$$C_n = \frac{1}{X_o}\int_{-\Delta X/2}^{X_o-\Delta X/2} X_o \sum_{r=-\infty}^{\infty}\left[\sum_{k=0}^{N-1} h(k\Delta X)\,\delta(x-k\Delta X-rX_o)\right] e^{-i2\pi nx/X_o}\, dx. \qquad \text{Equation 20}$$

One should notice that the period over which Equation 20, is evaluated has been shifted so that the ends of the period lie between adjoining samples. The reason for this will be explained later. Since the integral in Equation 20 is evaluated over one period, r=0 and the summation with respect to r drops out of the integral to give

$$C_n = \int_{-\Delta X/2}^{X_0 - \Delta X/2} \sum h(k\Delta x)\, \delta(x - k\Delta x)\, e^{-i2\pi n x/X_0}\, dx. \qquad \text{Equation 21}$$

Since h(kΔx) is a constant with respect to x, the summation of h(kΔx) is brought outside the integral to give

$$C_n = \sum_{k=0}^{N-1} h(k\Delta x) \int_{-\Delta X/2}^{X_0 - \Delta X/2} e^{-i2\pi n x/X_0}\, \delta(x - k\Delta x)\, dx. \qquad \text{Equation 22}$$

By definition

$$\int_{X_1}^{X_2} f(\alpha)\, \delta(\alpha - X_0)\, d\alpha = f(X_0), \qquad \text{Equation 23}$$

therefore

$$C_n = \sum_{k=0}^{N-1} h(k\Delta x)\, e^{-i2\pi n k \Delta x/X_0}\, dx. \qquad \text{Equation 24}$$

Since $X_0 = N\Delta x$, then

$$C_n = \sum_{k=0}^{N-1} h(k\Delta x)\, e^{-i2\pi n k/N} \qquad \text{Equation 25}$$

Substituting Cn back into Equation 15 (the Fourier transform of the periodic function $h^1(x)$), we get

$$H^1\left(\frac{n}{N\Delta x}\right) \sum_{n=-\infty}^{\infty} \sum_{k=0}^{N-1} h(k\Delta x)\, e^{-i2\pi n k/N}\, \delta\left(f - n\left(\frac{1}{N\Delta x}\right)\right). \qquad \text{Equation 26}$$

By definition

$$\delta\left(f - n\left(\frac{1}{N\Delta x}\right)\right) = 0 \quad for \quad f \neq \frac{n}{N\Delta x} \,, \qquad \text{Equation 27}$$

and the summation with respect to n drops out since the value of the delta funciton is zero everywhere except at $f = \frac{n}{N\Delta x}$ when it has the value of 1.0, and

$$H'\left(\frac{n}{N\Delta x}\right) = \sum_{k=0}^{N-1} h(k\Delta x)\, e^{-i2\pi nk/N} \,. \qquad \text{Equation 28}$$

Equation 28 is the discrete Fourier transform which in more general form is stated as

$$G\left(\frac{n}{N\Delta x}\right) = \sum_{k=0}^{N-1} g(k\Delta x)\, e^{-i2\pi nk/N} \,, \qquad \text{Equation 29}$$

where n=0, 1, 2, 3, 4, ... Δx is the sampling interval and N is the number of samples.[10]

Earlier it was graphically demonstrated that the discrete Fourier transform is a periodic function. To show this, replace n by r in Equation 29 so that

$$G\left(\frac{r}{N\Delta x}\right) = \sum_{k=0}^{N-1} g(k\Delta x)\, e^{-i2\pi(r+N)k/N} \,. \qquad \text{Equation 30}$$

It was shown that the period of the discrete Fourier transform was equal to the interval over which the function was sampled X_o and that there were N samples within that interval. Let r=r+N

$$G\left(\frac{r+N}{N\Delta x}\right) = \sum_{k=0}^{N-1} g(k\Delta x)\, e^{-i2\pi(r+N)k/N}$$
$$= \sum_{k=0}^{N-1} g(k\Delta x)\, e^{-i2\pi rk/N}\, e^{-i2\pi k} . \qquad \text{Equation 31}$$

By definition

$$e^{-i2\pi k} = \cos(2\pi k) - i\sin(2\pi k) \qquad \text{Equation 32}$$
$$= 1.0 \qquad \text{for k is any integer.}$$

Therefore

$$G\left(\frac{r+N}{N\Delta x}\right) = \sum_{k=0}^{N-1} g(k\Delta x)\, e^{-i2\pi rk/N} , \qquad \text{Equation 33}$$

and

$$G\left(\frac{r+N}{N\Delta x}\right) \equiv G\left(\frac{r}{N\Delta x}\right) . \qquad \text{Equation 34}$$

The discrete Fourier transform is a periodic function where one period is composed of N samples.[11]

In a similar manner the inverse Fourier transform can be derived. The inverse Fourier transform is defined as

$$g(k\Delta x) = \frac{1}{N}\sum_{n=0}^{N-1} G\left(\frac{n}{N\Delta x}\right) e^{i2\pi nk/N}$$ Equation 35

The discrete Fourier transform requires that the function being transformed, must be sampled at equidistant intervals. The fact that the discrete Fourier transform is a period function imposes a restriction on the rate at which the function must be sampled in order to minimize error.

Given that a function h(x) is continuous over all space and its Fourier transform, H(f), takes on the value of zero after some finite frequency fc, that function is defined to be bandlimited.[12] That is H(f) has a finite width of 2fc. It was shown previously that sampling a function caused its Fourier transform to become periodic. If a function is sampled at intervals of Δx, then it s Fourier transform becomes a periodic function with a period of $1/\Delta x$

h(x) S(x) H(f)*S(f)

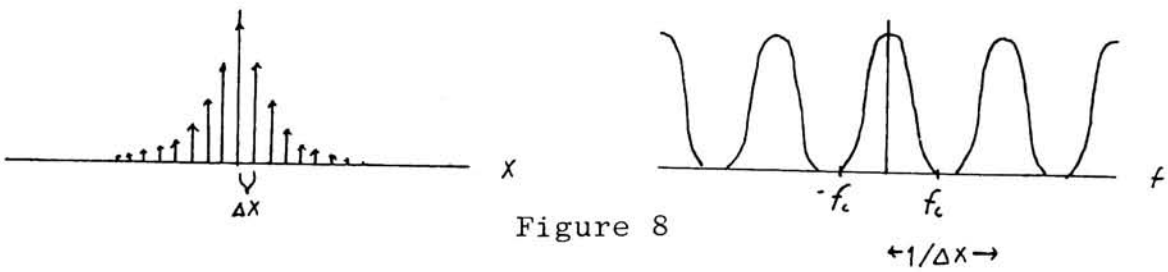

Figure 8

If the sampling rate is such as to cause the period of the transform of the sampled function to become less than $2f_c$, then the repetitions of H(f) will begin to overlap. This is known as aliasing.

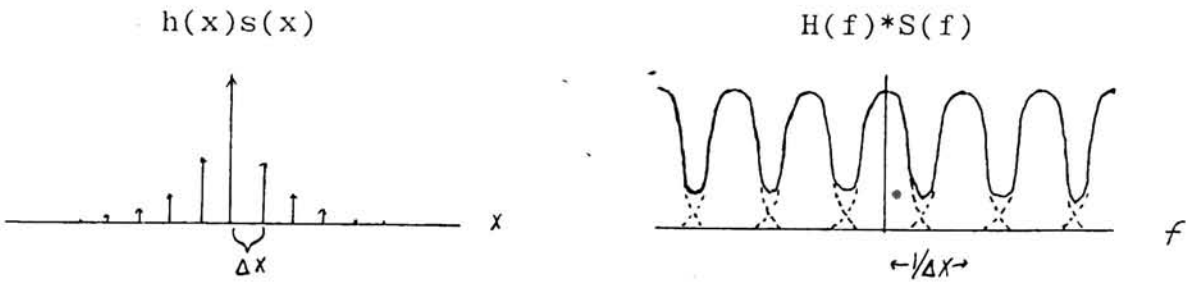

Figure 9

The values at the point of overlap is the sum of the two repetitions, and the Fourier transform is corrupted. In order to prevent aliasing the sampling rate must be

$$\Delta x \leq \frac{1}{2f_c}, \qquad \text{Equation 36}$$

for band-limited functions.[13, 14]

In most cases the function under examination is not band-limited, which means its Fourier transform is continuous. If the Fourier transform is continuous, then aliasing will always occur when computing the discrete Fourier transform. When convolving a continuous function with a series of equally spaced delta functions, overlap will take place no matter how far apart the delta functions are spaced. In

order to minimize aliasing in the region of interest, a cutoff frequency must be chosen after which no significant information is thought or known to exist. By setting this maximum frequency of interest equal to f_c, a minimum sampling rate is calculated using the relationship in Equation 36. By meeting this requirement aliasing should be insignificant throughout the region of interest. As a general rule, the higher the sampling rate the lower the error due to aliasing and the more accurate the results will be.

Another consideration when applying the discrete Fourier transform is the truncation interval which is used. The interval over which the function is sampled, determines the spacing of the frequencies computed by the discrete Fourier transform. If the function is sampled over an interval of X_0, then the frequencies will be reported every $1/X_0$ units. That is

$$\Delta f = 1/X_0. \qquad \text{Equation 37}$$

From the width of the truncation interval, the number of samples required can be calculated from the fact that

$$X_0 = N\Delta x \text{ or } N = X_0/\Delta x. \qquad \text{Equation 38}$$

Since $\Delta f = 1/X_0$ and $X_0 = N\Delta x$ then

$$1 = N\Delta x\Delta f. \qquad \text{Equation 39}$$

This defines the relationship between the number of samples, the sampling rate and the spacing between the reported frequencies. Using Equation 39 and $\Delta x \leq 1/2f_c$, then all the parameters for proper sampling and truncation can be determined.

A final requirement for computing the discrete Fourier transform is that the end points of the truncation function do not coincide with the position of a sample value. The reason for this, is the fact that the sampled truncated function is periodic, as shown earlier. If the end points of the truncation function coincides with the position of a sampled value then time domain aliasing will occur. This results from the fact that the N^{th} point of one period will coincide and add to the first point of the next period. Therefore the end points of the truncation function should always be placed between adjoining sample values.[15]

When applying the discrete Fourier transform one should be aware of certain properties. If a function is sampled using N number of samples, then the computation of the discrete Fourier transform will result in N frequencies. The discrete Fourier transform produces a real and an imaginary part. The real part will be a function symmetric about the point n=N/2, while the imaginary part will be an odd function with respect to the same point. The modulus of the transform

is also a symmetric function about n= N/2. What is occurring is that the results from n= N/2 to N represent the negative frequencies of the transform. Because of this, only N/2 frequencies are actually reproted. Also of interest is the fact that every frequency is repeated except at f=0.[16] To calculate the discrete inverse Fourier transform, the real and imaginary parts must be in the form described above, otherwise error will result.[17]

From the mathematical expression for the discrete Fourier transform (Equation 29) it can be shown that $G(\frac{n}{N\Delta X})$ results from N^2 complex multiplications and N(N-1) complex additions.[18] Even when done by computer, computation can become very time consuming, especially if the number of points is large. Out of the need for a fast, efficient means of computing the discrete Fourier transform, James W. Cooley and John Tukey in 1965 produced what is now known as the Fast Fourier Transform (FFT).[19] By means of matrix factorization the FFT is able to reduce the number of complex operations to $N \log_2 N$. Because the number of operations is reduced, the time and cost of computing the Fourier transform is also reduced. A good example of this is the computation of the transform of 8192 samples which takes three quarters of an hour on an IBM 7094 by conventional computation. Using an FFT algorithm the same calculation takes only 5 seconds on the same machine.[20] The discrete

Fourier transform is now almost always computed using an FFT algorithm.

Experimental -

The images used in this work were those of an edge and a bartarget. These images were selected on the basis that they are easily represented as a function of one dimension. They were also selected because the eye views an image as a series of relative differences in transmission or reflectance. An edge and a bartarget are very simple examples where the differences between adjacent regions are used to define the quality of an image.

A National Bureau of Standards standard edge and a United States Air Force - 1951 transmission test target were contact printed onto Kodak Plus X film, which was processed according to manufacturer recommendations. Kodak Plus X film was selected because it is a fairly fine-grained film capable of producing a clean, noise-free image.

All measurements were made in transmission. Transmission was chosen instead of density because transmission is a fundamental physical quantity. Before scanning the image with the microdensitometer, several parameters had to be calculated in order to properly set up the instrument so that a linear response was achieved. If the microdensitometer is not set up properly in regard to geometry, partial coherence,

depth of focus, flare, slit alignment and substrate scattering, then a non-linear response may result causing the proper interpretation of results to become impossible. The theory of linear microdensitometry is beyond the scope of this paper. The parameters used and their means of calculation are thoroughly described in "Microdensitometer Optical Performance: Scalar Theory and Experiment", Richard E. Swing, Optical Engineering, November-December 1976, Vol. 15, No. 6. A Zeis SMP05 microdensitometer was used to scan the images, having been set up for image scanning with overfilled optics using incoherent illumination.

Illumination was provided by a tungsten source with a green filter in the light path, which effectively produced a monochromatic illumination of 500 nm wavelength. The required minimum numerical aperture for the efflux objective was calculated to be 0.075. A 0.1NA objective was used for the efflux objective. A minimum numerical aperture of 0.125 was calculated for the influx objective and a 0.2NA objective was used. A sampling aperture of 5μm was calculated to be the minimum usable aperture width. However, since a 5μm slit is capable of resolving information out to 200 cycles/mm (f max= 1000/slit width, f max= $1000/_{5}$μm= 200 cycles/mm) and the film was judged not to contain information past 100 cycles/mm, a 10μm slit was used instead.

Using the sampling criteria of $\Delta x \leq 1/2f_c$, and having decided on 100 cycles/mm as the maximum frequency of interest, a maximum sampling interval of 5μm was calculated. A minimum frequency resolution of 1 cycle/mm for the Fourier transformer was chosen. From $\Delta f = 1/X_0$ a minimum scan length of 1 mm was found to be required. The edge was scanned over a 1 mm interval taking measurements every 5μm, while Group 8, Element 5 of the resolution test target was scanned over a 1.35 mm interval (in order to scan the entire image) using the same sampling rate. This produced a 200 sample representation of the edge and a 270 sample representation of the bartarget.

When an object is scanned with a microdensitometer, its image is modified or degraded by the modulation transfer characteristics of the instrument. Unless the microdensitometer contains a perfect imaging system (has a flat MTF), then the image will be a degraded representation of the object. The problem is to recover the original object from the image knowing something about the response of the system. In this work the microdensitometer was set up to produce a linear response. Because of this, the Fourier transform of the original object, O(f), can be recovered by means of inverse filtering.[21] O(f), can be found by dividing the Fourier transform of the image, I(f), by the frequency response of the microdensitometer H(f). That is,

since

$$I(f)= O(f)\ H(f) \qquad \text{Equation 40}$$

for a linear system, then

$$O(f)= \frac{I(f)}{H(f)}. \qquad \text{Equation 41}$$

Once O(f) has been calculated, then the original object can be reconstructed by computing the inverse Fourier transform of O(f).

The frequency response of the microdensitometer can be approximated by the product of the MTF of the efflux objective and the frequency response of the scanning slit,[22] if the microdensitometer is of high quality and has been set up properly as in this work. The efflux objective was a diffraction limited lens which means its MTF is defined as

$$MTF(f)= \frac{2}{\pi}\left(\phi - \cos(\phi)\sin(\phi)\right), \text{ where } \phi = \cos^{-1}(f/f_c) \qquad \text{Equation 43}$$

and f_c is the cutoff frequency of the lens, which in this case was calculated to be 400 cycles/mm. Let $u=f/f_c$ then

$$MTF(f)= \frac{2}{\pi}\left(\cos^{-1}(u) - u\sqrt{1-u^2}\right). \qquad \text{Equation 44}$$

Expansion of Equation 44 into a power series can easily be accomplished. Using only the first three terms of the expansion of each term and then collecting terms produces

$$MTF(f) = 1 - \frac{4}{\pi} u + \frac{1}{\pi} u^2$$

$$= 1 - \frac{4}{\pi}\left(\frac{f}{f_c}\right) + \frac{1}{\pi}\left(\frac{f}{f_c}\right)^2 . \qquad \text{Equation 45}$$

Equation 45 is a very close approximation to Equation 43 and much simpler to implement.[23] The transmission characteristics of the scanning slit can be mathematically defined by a rectangle function. The Fourier transform of a rectangle function is a sinc function and so the frequency response of the scanning slit is a sinc function. For a 10μm wide slit the frequency response is

$$F[\text{scanning aperture}] = \frac{\sin(0.01\pi f)}{\pi f} . \qquad \text{Equation 46}$$

The product of Equations 45 and 46 is a very good approximation to the frequency response of the microdensitometer, therefore

$$H(f) = \left(1 - \frac{4}{\pi}\left(\frac{f}{f_c}\right) + \frac{1}{\pi}\left(\frac{f}{f_c}\right)^2\right) \frac{\sin(0.01\pi f)}{\pi f} \qquad \text{Equation 47}$$

A problem arises when calculating the Fourier transform of the original object from Equation 41. H(f), as shown in Equation 47 is the product of a sinc function and another function. The sinc function in Equation 46 falls off to zero at 100 cycles/mm causing I(f) to be divided by very tiny quantities as f approaches 100 cycles/mm. This creates a very large error in the high frequencies of O(f). To get around

the problem of dividing I(f) by very tiny numbers, the frequency response of the microdensitometer H(f), is set equal to a constant after falling to a specific amplitude.[24] In this work H(f) was set equal to 0.25 for all frequencies greater than 75 cycles/mm, 0.25 being the value of H(f) at that frequency. By doing this, important information at low frequencies is restored without introducing a large error at the higher frequencies where little or no significant information exists.

All data was stored and processed by the RIT Xerox Sigma 9 computer. The Fourier transforms of the images were computed with an FFT program capable of handling any number of data points, not just 2^n number of points which most FFT are only capable of handling. This allowed a convenient number of samples to be used. When taking the forward Fourier transform the image data had to be transformed into a series of complex numbers. This was done by setting the data equal to the real part and setting the imaginary part equal to zero. When computing the inverse Fourier transform the real and imaginary part of the transform had to be specified in the form described previously, and then the complex conjugate computed before using the FFT program. The modulus of the Fourier transform of the data was normalized to 1.0 by dividing by the value of the transform at f=0. The modulus of the inverse Fourier

transform (computed when reconstructing the images) was normalized by dividing by the number of points in order to preserve the original magnitude of the data defining the images.

The Fourier transforms of the images were first filtered using ideal low and high pass filters. The images were then reconstructed by computing the inverse Fourier transform of the filtered image transforms. Filtering was accomplished by multiplying the Fourier transform of the image by a filter function H(f). That is

$$G(f)=I(f)H(f), \qquad \text{Equation 48}$$

where G(f) is the filtered transform, I(f) the Fourier transform of the original image and H(f) the filter function. The ideal low pass filter (ILPF) is a rectangle function originating at f=0. The ILPF is defined as

$$H(f)=\begin{cases} 1 & |f| \leq f_c \\ 0 & |f| > f_c \end{cases} \qquad \text{Equation 49}$$

where f_c is the cutoff frequency.

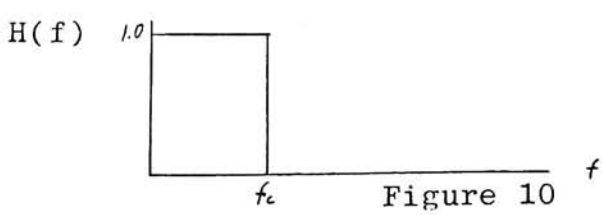

Figure 10

By applying the ILPF, the magnitude of all frequencies less than f_c are unchanged while the magnitude of those frequencies greater than f_c becomes zero. The cutoff frequency of the ILPF was decreased from f=100 cycles/mm to f=0 cycles /mm in increments of $5\Delta f$ for each image. The ideal high pass filter (IHPF) is also a rectangle function, however it originates at the highest frequency contained in the transform, in this case 100 cycles/mm, and ends at some cutoff frequency.[26] The IHPF is defined as

$$H(f)=\begin{cases} 1 & |f| \geq f_c \\ 0 & |f| < f_c \end{cases} \qquad \text{Equation 50}$$

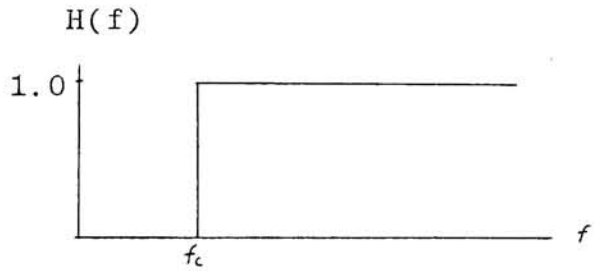

Figure 11

When applying the IHPF the magnitude of the frequencies less than f_c becomes zero while those frequencies greater than f_c remain unaffected. The cutoff frequency of the IHPF was increased at intervals of $20\Delta f$ from f=0 until the images were totally obliterated.

The image transforms were next filtered using exponential low and high pass filters. The exponential filter is a smooth filter. Rather than having a sharp cutoff the exponential filter causes attenuation to be done more gradually. The cutoff frequency is specified as that frequency at which the filter equals a specific value. In most cases the value of the filter at the cutoff frequency is specified to be $1/\sqrt{2}$ of the maximum value of the filter which is usually 1.0. The exponential low pass filter (ELPF) causes the amplitude of the higher frequencies to be decreased relative to the lower frequencies. The ELPF is defined as

$$H(f) = e^{[\ln(1/\sqrt{2})](f/f_c)^n}$$

$$= e^{-0.347(f/f_c)^n} \qquad \text{Equation 51}$$

27

where n controls the rate at which the filter falls off. In this work n was set equal to 2.

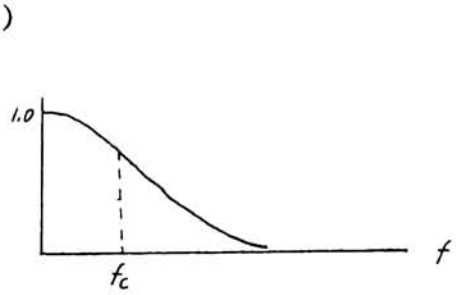

Figure 12

The ELPF was used for various cutoff frequencies, starting from f= 5Δf and ranging to f=40Δf. The exponential high pass filter (EHPF) is very similar to the ELPF, except it is reflected about f=0 and shifted to the right. This causes the amplitude of the low frequencies to be reduced to a much larger extent than that of the higher frequencies. The EHPF is defined by

$$H(f) = e^{-0.347\left(\frac{f_0 - f}{f_c}\right)^n}, \qquad \text{Equation 52}$$

where f_0 is the desired starting frequency of the filter (the maximum frequency reported by the transform). In this case f_0=100 cycles/mm and again n=2. The value of the cutoff frequency of the EHPF was ranged from f=80Δf to f=20Δf.

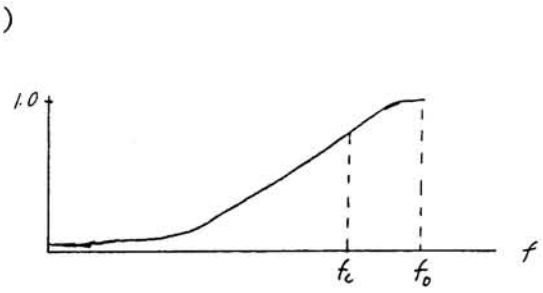

Figure 13

Another filter similar to the EHPF was used, this one being a high frequency emphasis exponential high pass filter. This filter does not attenuate the amplitude of the lower frequencies but rather boosts or magnifies the amplitude of the higher frequencies. This is done by adding a constant to the EHPF. The high frequency filter used, is defined as

$$H(f) = \frac{1.0}{1.0 + e^{-0.347\left(\frac{f_0 - f}{f_c}\right)^n}}$$ Equation 53

where again n=2, and f_0=100 cycles/mm.

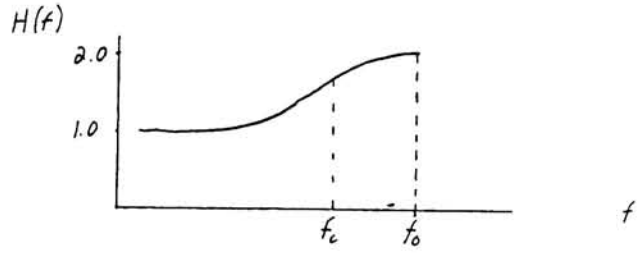

Figure 14

This filter was used on the Fourier transforms of the degraded images of the edge and bartarget for various frequencies. The idea being to enhance the degraded images by increasing the amplitude of the higher frequencies.

The effect of aliasing was investigated by sampling the image data at various increments other than one, and then computing the Fourier transform. The resulting transform was then compared to the original transform of the image at the same frequencies in order to detect any changes due to aliasing. The image data was sampled by taking every other point, every third point and every fourth point. Since the total width over which the function was sampled remained constant the interval between the frequencies reported stayed the same so that valid comparison could be made between the different transforms. Only the number of frequencies reported was modified by the coarser sampling rates employed.

Results

The Fourier transforms of the edge and the bartarget were corrected for the frequency response of the microdensitometer. The result was to cause the value of the transforms to increase slightly at low frequencies (5% at 10 cycles/mm) and to increase to a very large extent at high frequencies (up to 300% at 99 cycles/mm). The microdensitometer has a limiting response and will cause attenuation at all frequencies. Attenuation will be greater at high frequencies since the response of the instrument drops off as the frequency of the input signal increases. Because of this, the greatest change in the corrected Fourier transforms of the images will occur at higher frequencies. It should be noted that the largest increases in the corrected transforms took place at high frequencies, the magnitude of those frequencies was so small compared to that of the low frequencies that the relative change in magnitude of the high frequencies was for the most part insignificant. The images produced from the corrected Fourier transforms demonstrated no significant change from the original images other than a slight increase in noise which may well be as much of a result of error due to calculation as from the increased magnitude of the higher frequencies.

Correction for the frequency response of the microdensitometer did produce a difference in the reconstructed image,

that being in the end points of the images of the edge. This error does not occur in the corrected image of the bartarget. A test was conducted wherein the orignal data from scanning the edge and the bartarget was Fourier transformed and then the resulting function inverse Fourier transformed. The resulting images should be identical to the originals. The image of the bartarget showed no significant change. The edge however, demonstrated the same error at the end points (an oscillation of increasing magnitude) encountered before, but to a lesser degree. An error is being introduced into the image by the calculation of the discrete Fourier transform. The discrete Fourier transform treats the sampled function as a periodic function. The bartarget used is a periodic type function, terminating at the same level from which it originated after several identical cycles. The edge however, contains a large discontinuity. That is, after starting at a low level of transmission it increases in value and then levels off at some higher level of transmission where it terminates. The function never returns to its original starting values and so contains a large discontinuity. Figure 15 demonstrates how the discrete Fourier transform views an edge or step function.

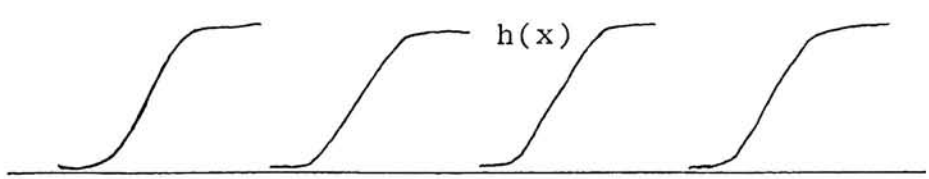

Figure 15

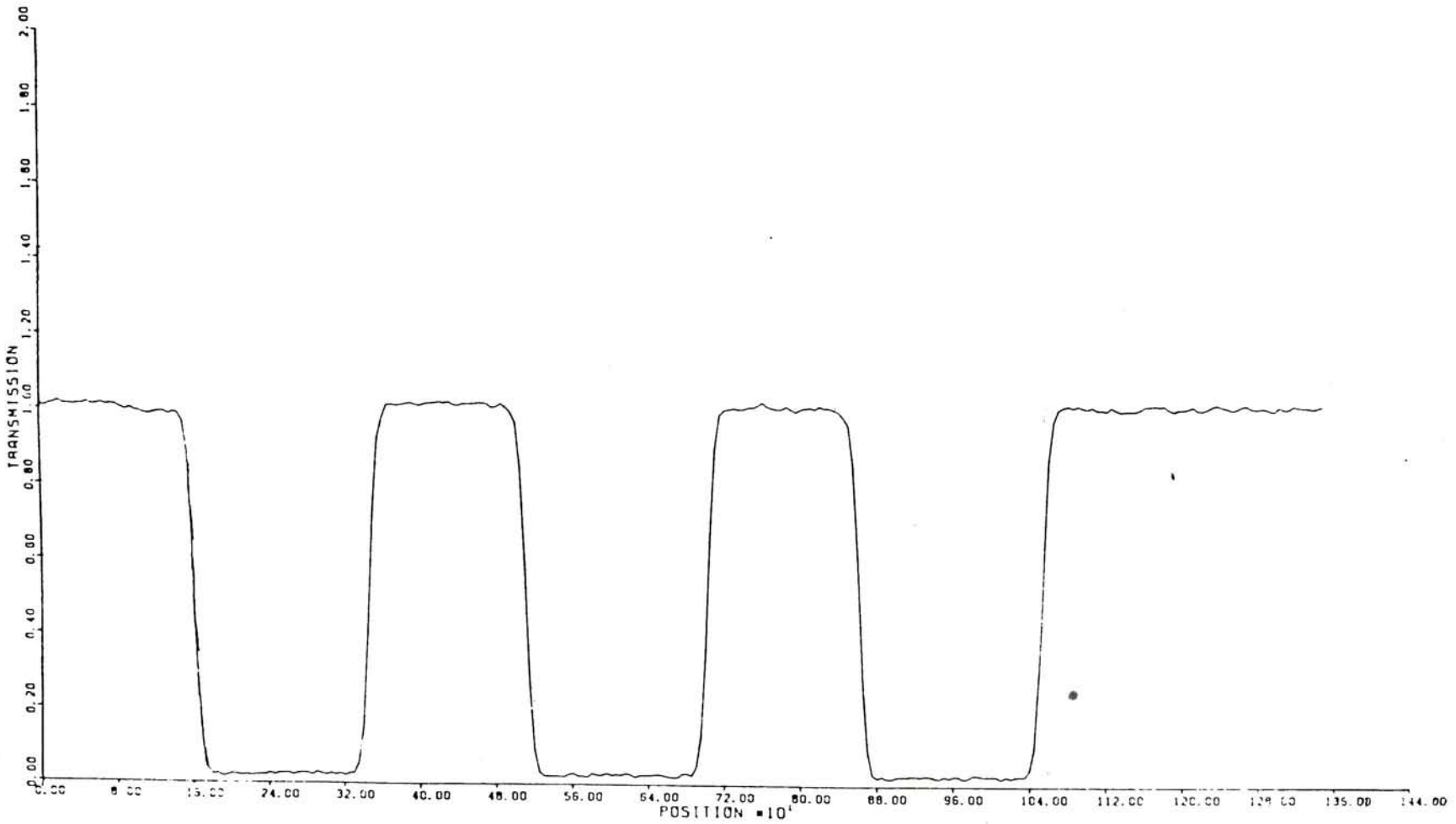
TRANSMISSION
2.00
1.80
1.60
1.40
1.20
1.00
0.80
0.60
0.40
0.20
0.00
8.00
16.00
24.00
32.00
40.00
48.00
56.00
64.00
72.00
80.00
88.00
96.00
104.00
112.00
120.00
128.00
136.00
144.00
POSITION *10⁴

BARTARGET-

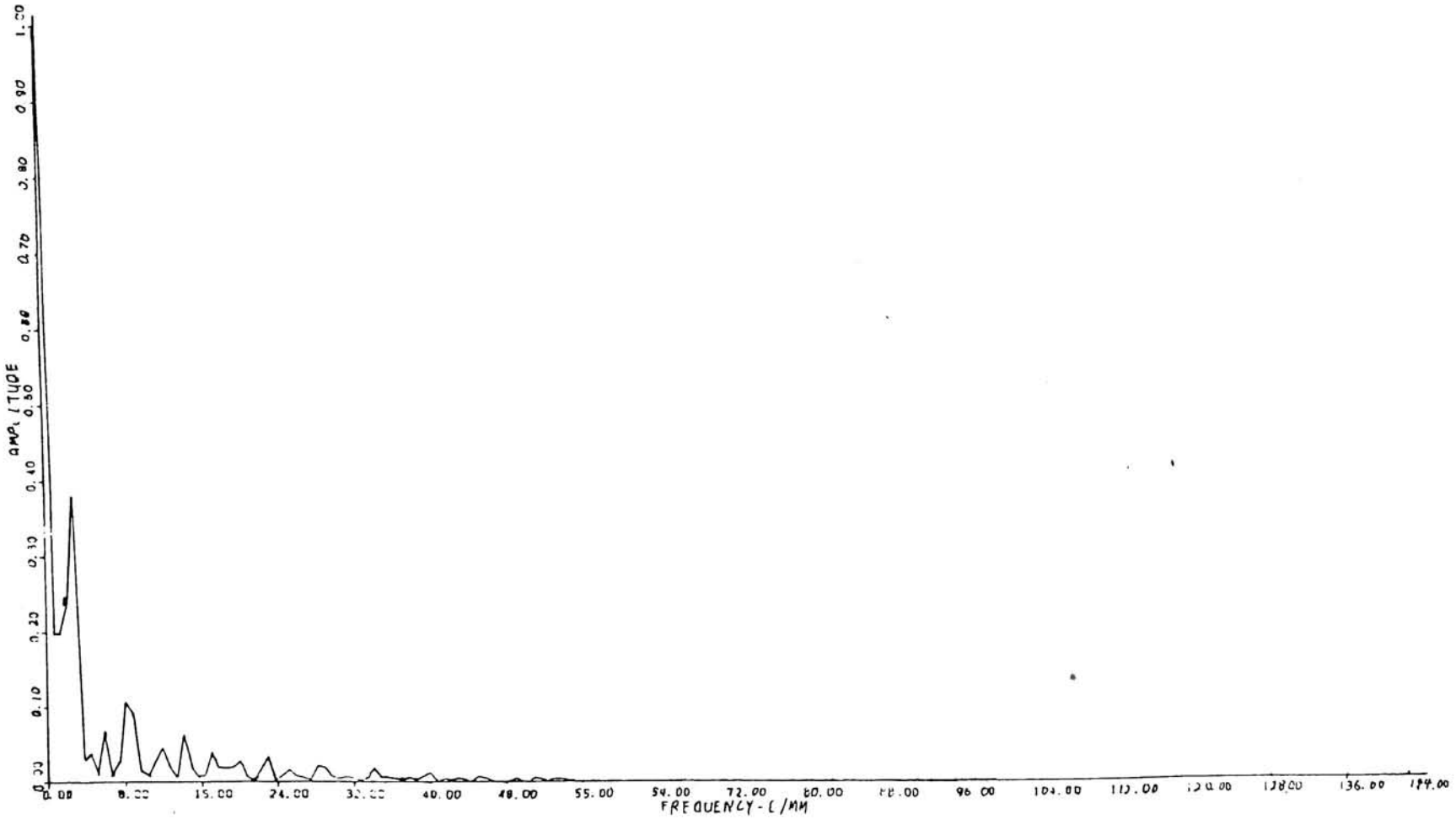

BARTARGET- Amplitude Spectrum

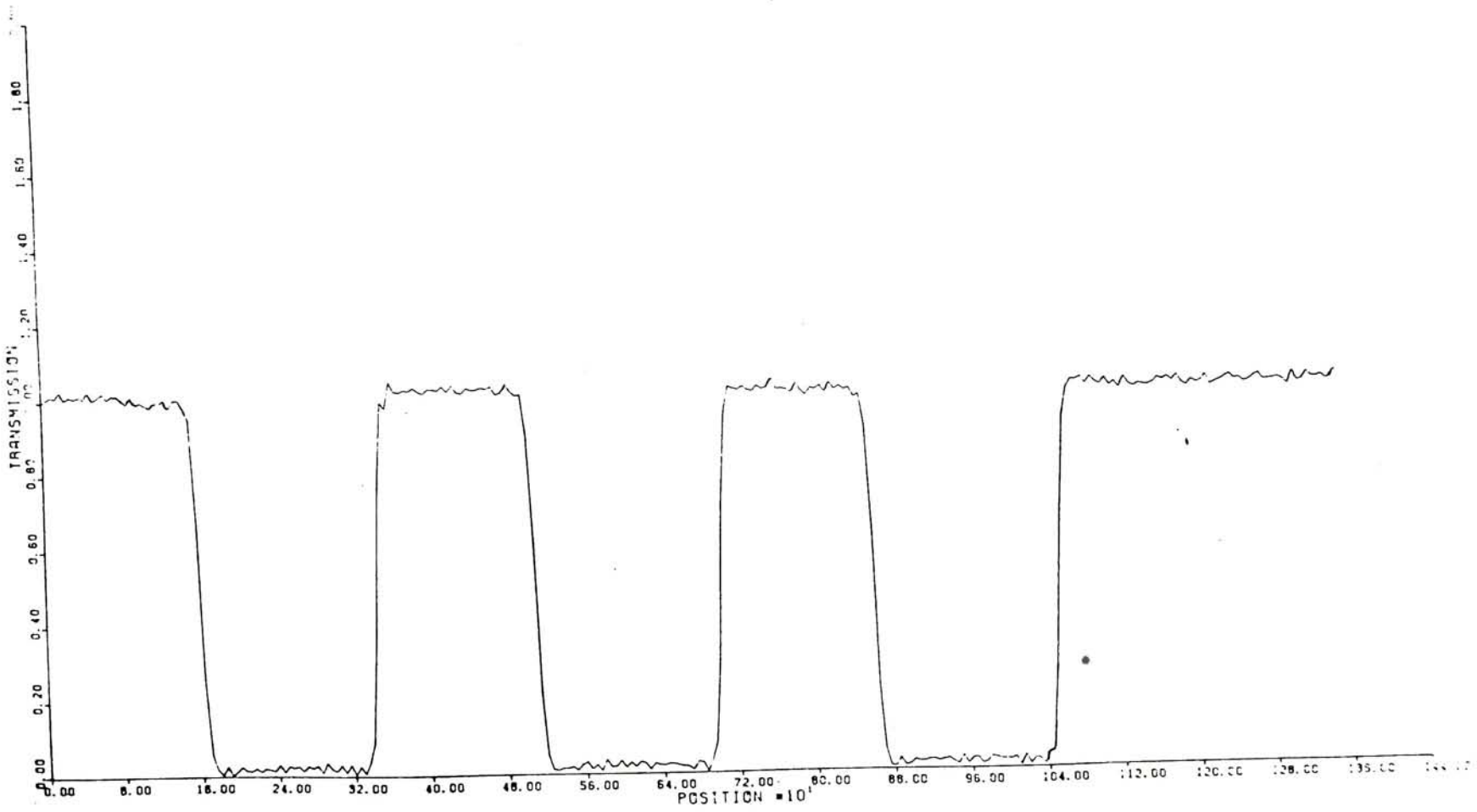

BARTARGET- Corrected For Response Of Microdensitometer

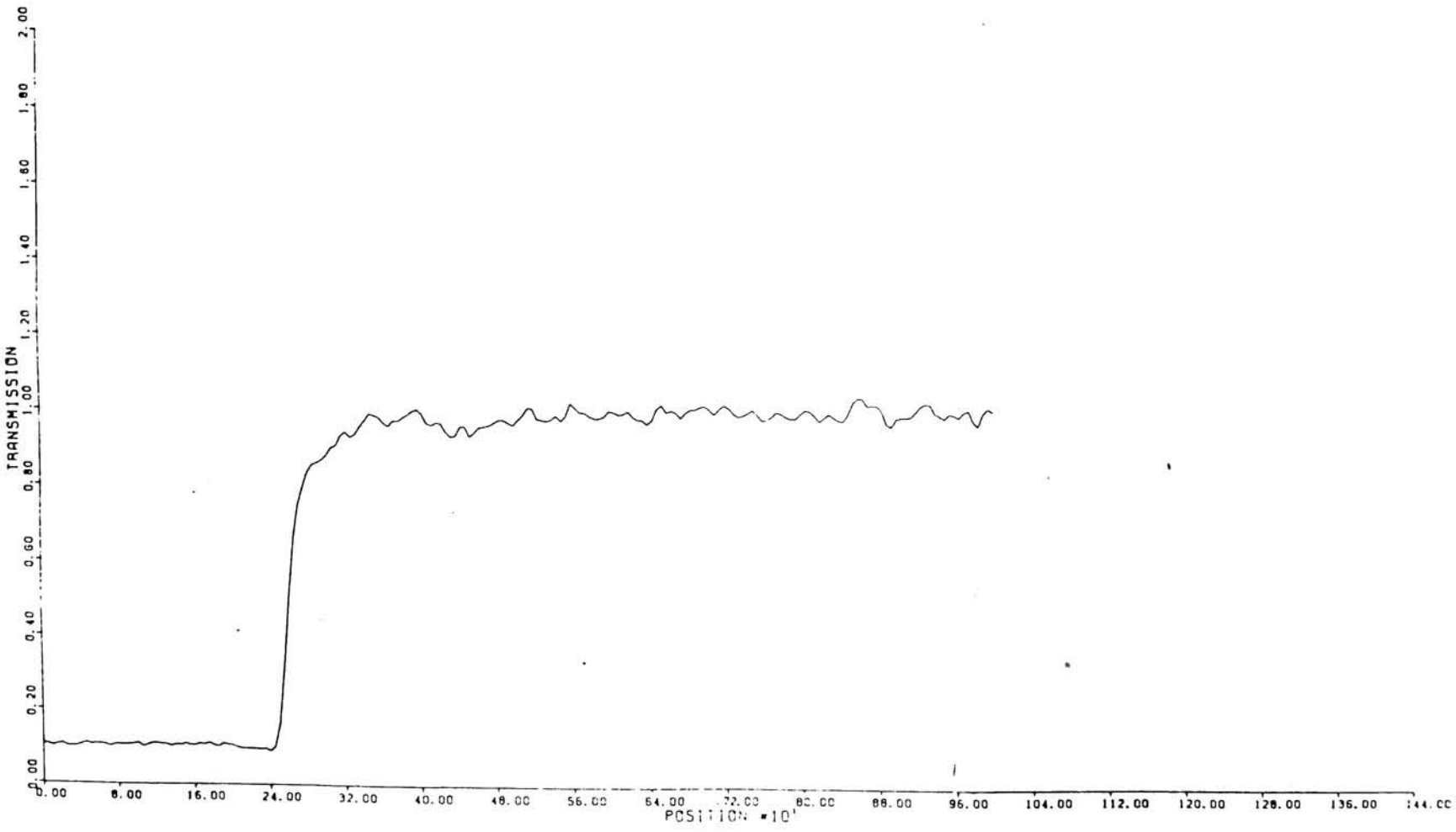
TRANSMISSION
0.00
0.20
0.40
0.60
0.80
1.00
1.20
1.40
1.60
1.80
2.00
0.00
8.00
16.00
24.00
32.00
40.00
48.00
56.00
64.00
72.00
80.00
88.00
96.00
104.00
112.00
120.00
128.00
136.00
144.00
POSITION *10'

EDGE-

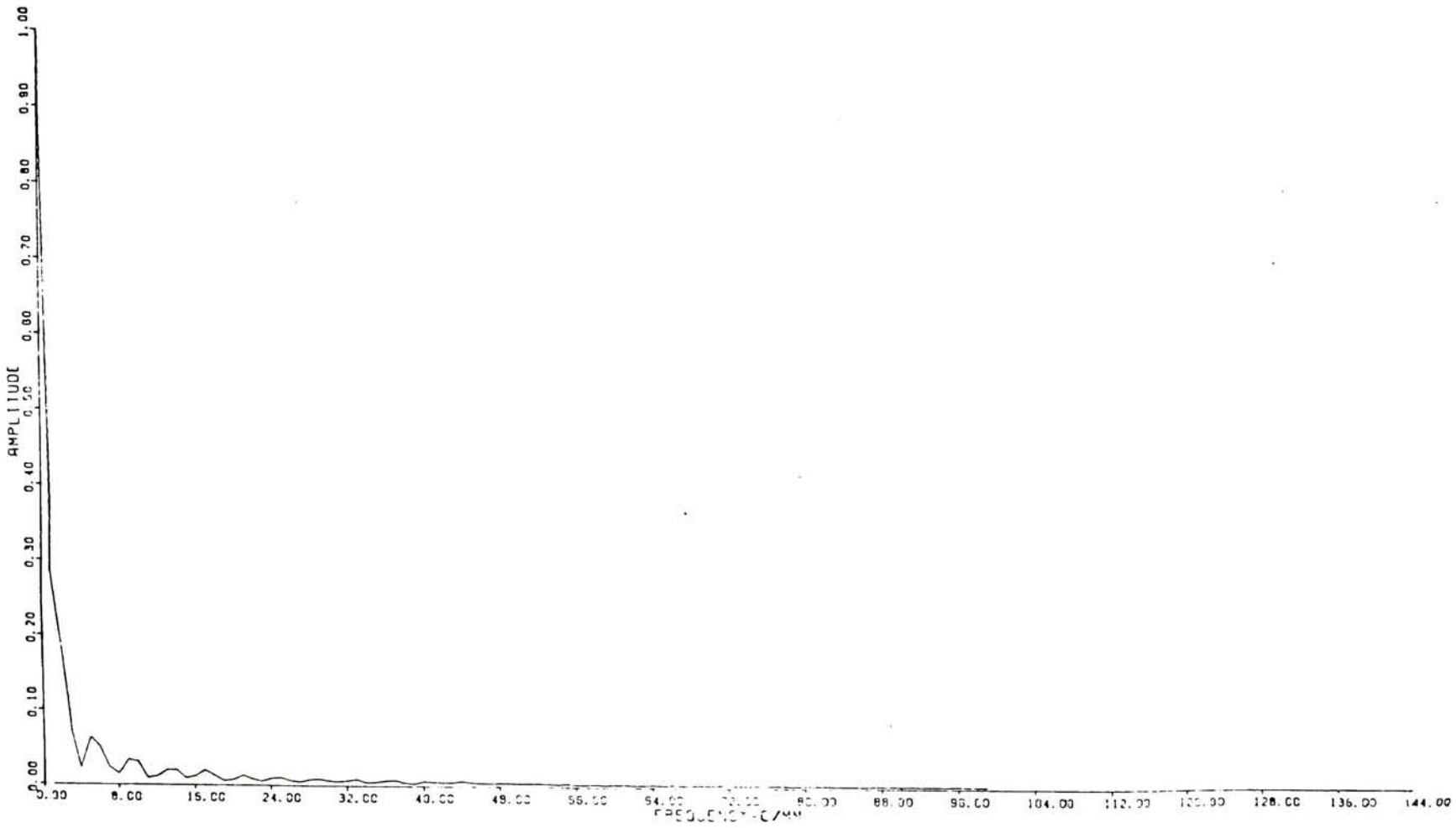

EDGE- Amplitude Spectrum

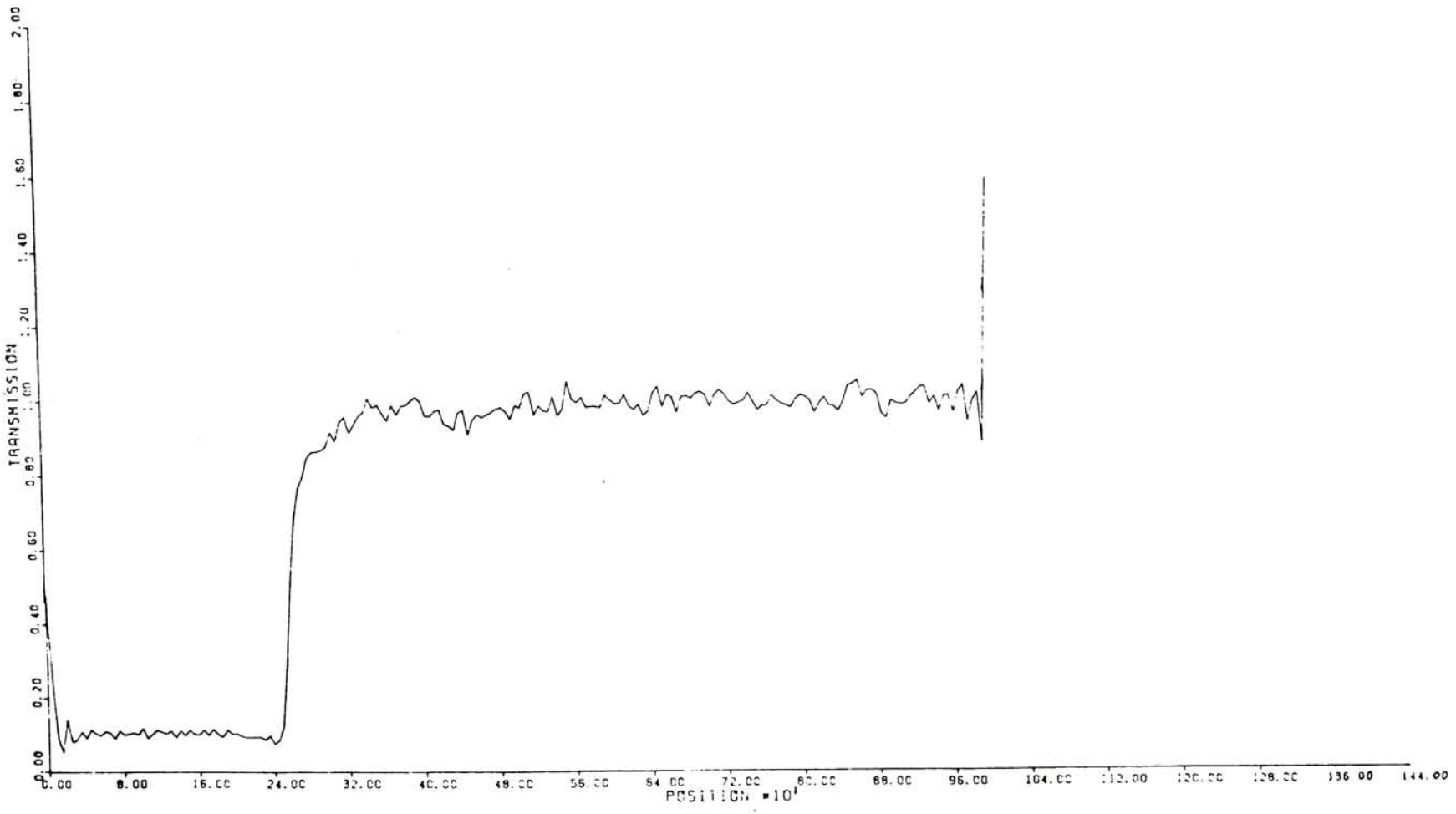

EDGE- Corrected For Response Of Microdensitometer

Note that Figure 15 is not a continuous function. The discontinuity in the edge results in the error produced in the end points of the reconstructed images. As the amplitude of the higher frequencies increases the greater the error produced at the end points as is evidenced by the image produced from the corrected Fourier transform of the edge.

The ILPF has some interesting effects on the images of the bartarget and the edge. The filtered images of the bartarget demonstrate no significant changes until a cutoff frequency of about 80 cycles/mm was reached. At $f_c \approx 30$ cycles/mm the image is becoming much smoother and the edges are losing sharpness. Ringing is increasing as the cutoff frequency is decreased. Finally at $f_c \approx 15$ cycles/mm the image is almost unacceptable and at $f_c \approx 5$ cycles/mm is completely destroyed. The edge goes through a similar transition as the cutoff frequency of the ILPF is decreased. No significant change in the image occurs until f_c is approximately 50 cycles/mm. "Ringing" becomes very evident at $f_c \sim$ 40 cycles/mm. Smoothing and "ringing" increases until the image of the edge is all but obliterated at a cutoff frequency equal to 5 cycles/mm. In the images of the edge, the error at the end points increases as f_c decreases.

As the cutoff frequency of the ILPF is decreased, the noise in the images is reduced and the images become smoother. As suspected, no significant information was found to exist

past 75 cycles/mm. This is demonstrated by the fact that the amplitude of the transforms is very small at frequencies greater than 75 cycles/mm and that reducing it to zero in that region had no significant effect on the images. Of interest, is the effect that takes place in the images as the cutoff frequency is reduced. By the convolution thorem, the Fourier transform of the product of two functions is the convolution of their Fourier transforms. As is well known the convolutions of two funcitons results in a third much smoother function. When the cutoff frequency is decreased the amount of smoothing of the final image increases. This is a result of the fact that as a function becomes narrower in one domain, its corresponding function in the other domain increases in width. Therefore as f_c decreases, the width of the Fourier transform of the filter increases causing more smoothing to occur when it (the Fourier transform of the filter) is convolved with the image. "Ringing" is a result of the fact that the ILPF is a rectangle function whose Fourier transform is a sinc function. The sinc function is not a smoothly decreasing function but rather, contains side-lobes which create "ringing" when the function is convolved with the image. As the width of the rectangle function which defines the ILPF decreases with decreasing values of f_c, its Fourier transform increases in width causing the side-lobes of the transform to increase in width also. This in turn causes the amplitude and period of the "ringing to increase.

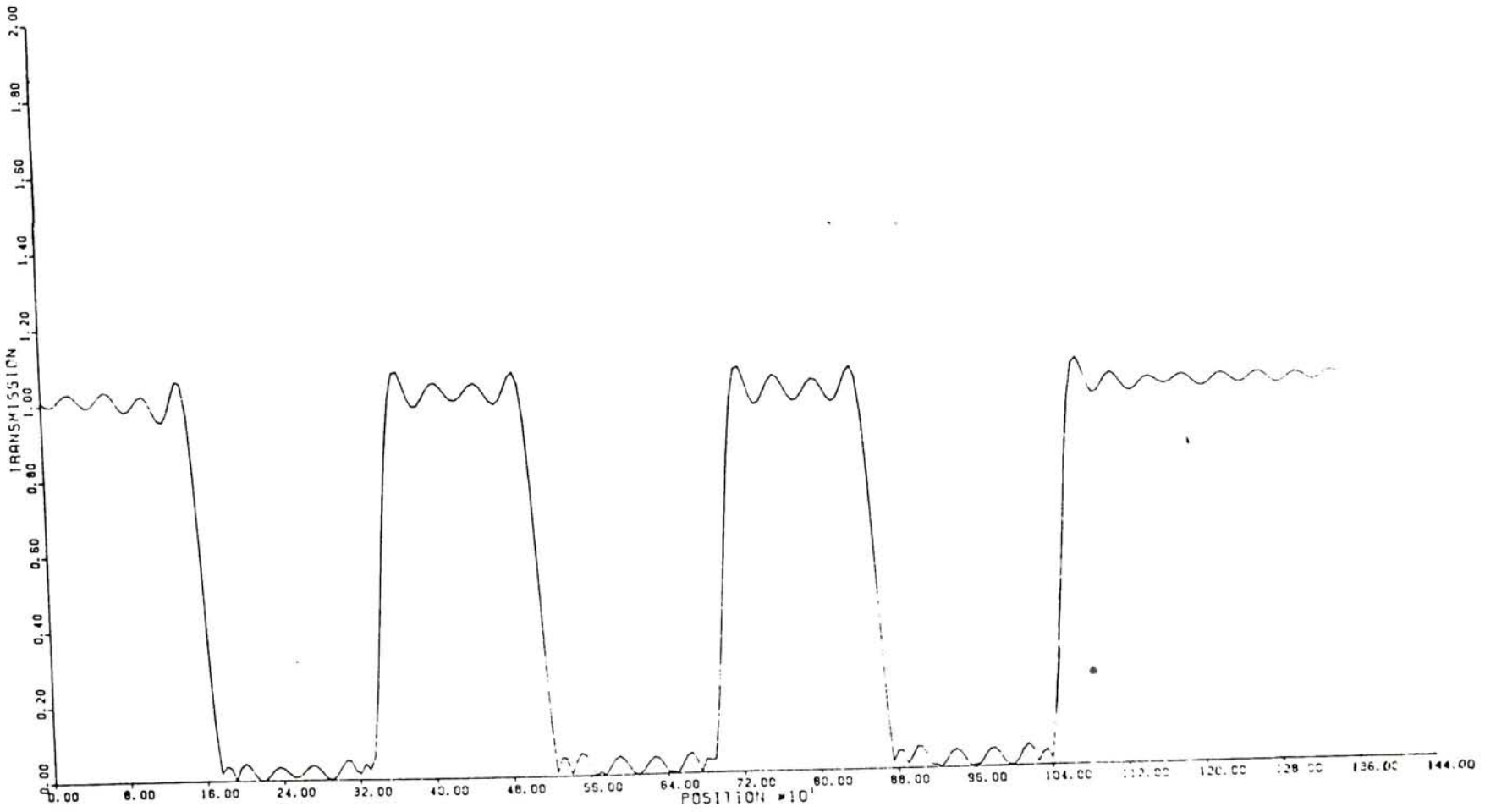

BARTARGET- Ideal Low Pass Filter, f_c= 25 cycles/mm

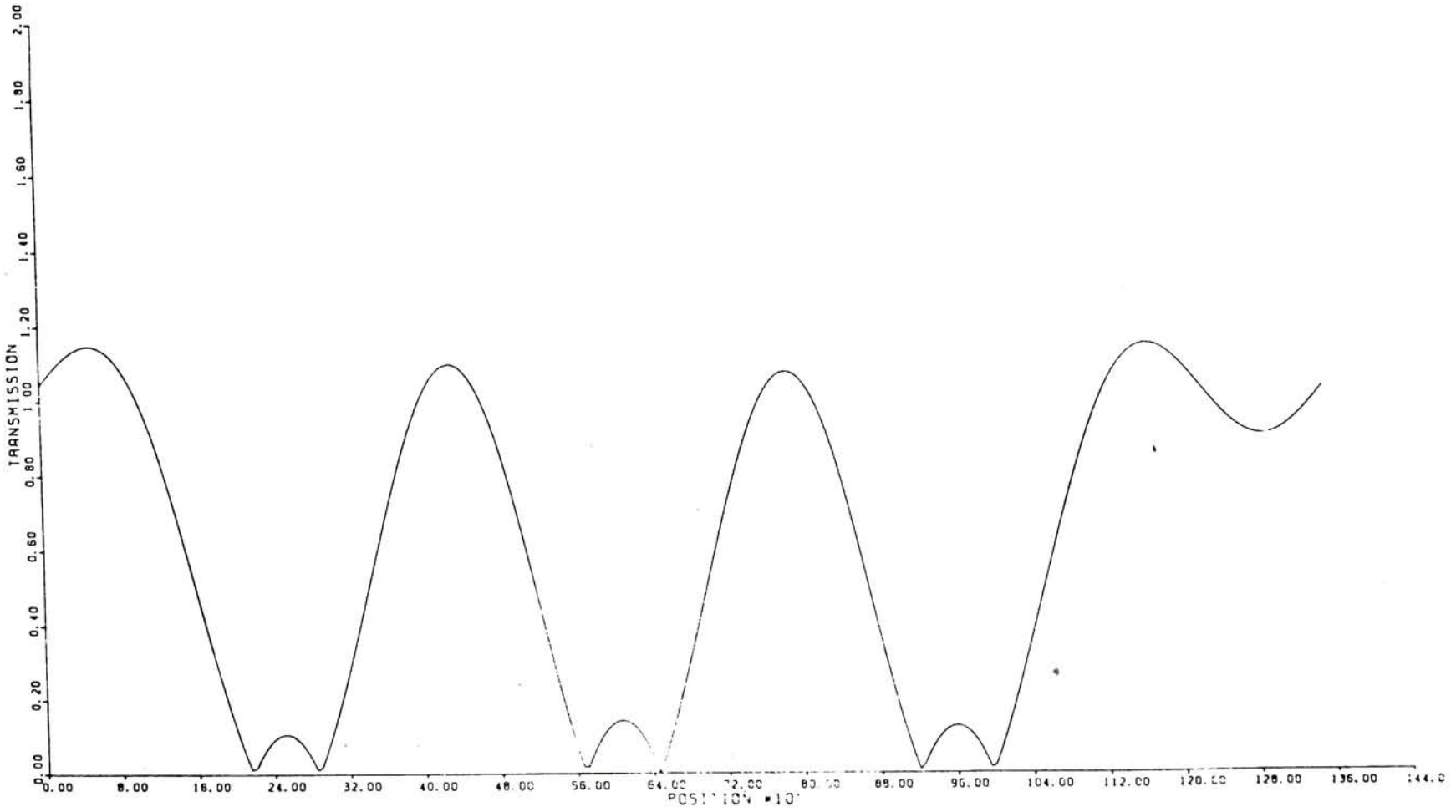

BARTARGET- Ideal Low Pass Filter, f_c= 3 cycles/mm

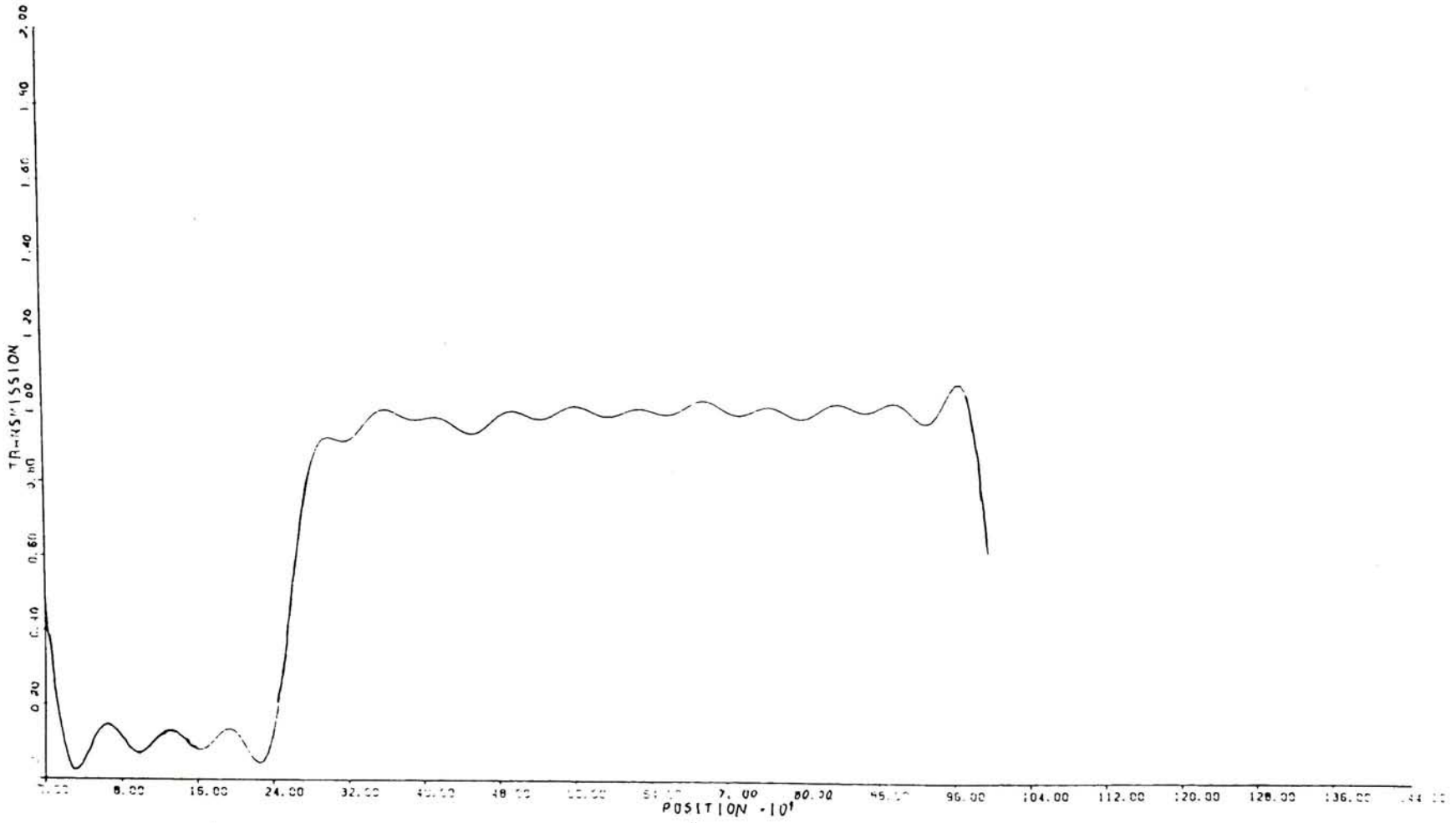

EDGE- Ideal Low Pass Filter, f_c= 15 cycles/mm

The results of the application of the IHPF are harder to analyze. When the amplitude of the initial frequency at f= 0 is reduced to zero both images preserved much of their original information except that the level of the signal in each is reduced, and those regions which originally had low transmission, become much higher in transmission, even greater than those regions which originally possessed high transmissions. This effect occurs throughout all cases where the IHPF is used and the image is not totally obliterated. As the cutoff frequency is increased, the average level of the signal is reduced and noise becomes more dominant in the images. Also as the cutoff frequency is increased only sharp transitions are preserved while the general shape of the image is destroyed. Edges remain sharp. Information about sharp transitions must therefore be contained at the higher frequencies of the transform since the amplitude of the low frequencies have been reduced to zero. The level of the signal in the filtered images is reduced because the amplitude of the frequencies unaffected by the filter is small. The level of the signal is therefore dependent upon the absolute magnitude of the frequencies of which it is comprised. As the cutoff frequency is increased, the magnitude of the noise stays practically the same. However, the magnitude of the noise relative to the signal increases since the level of the signal is reduced as f_c increases. The signal to noise ratio decreases when the IHPF is used. This

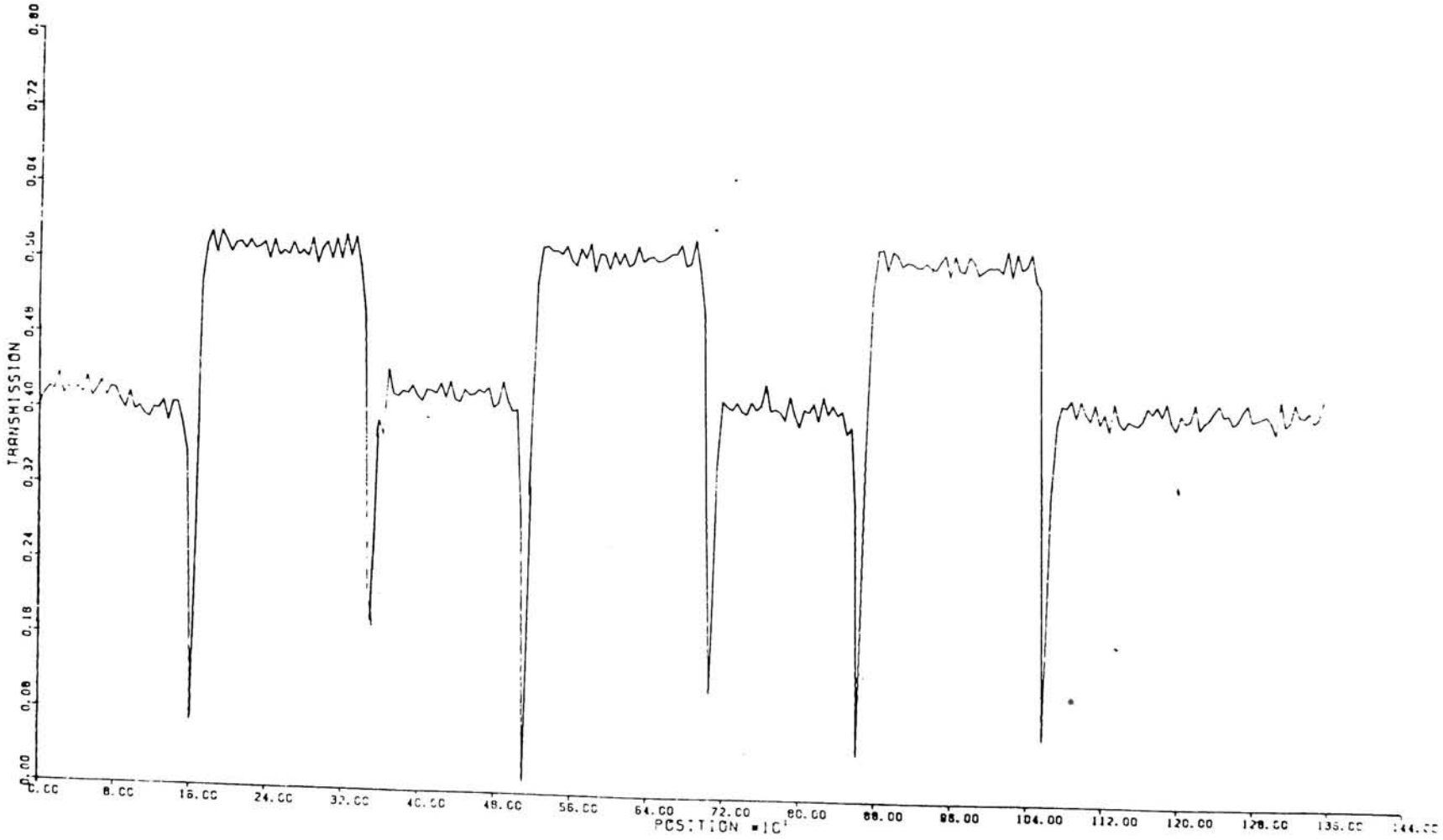

BARTARGET- Ideal High Pass Filter, f_c= 1 cycle/mm

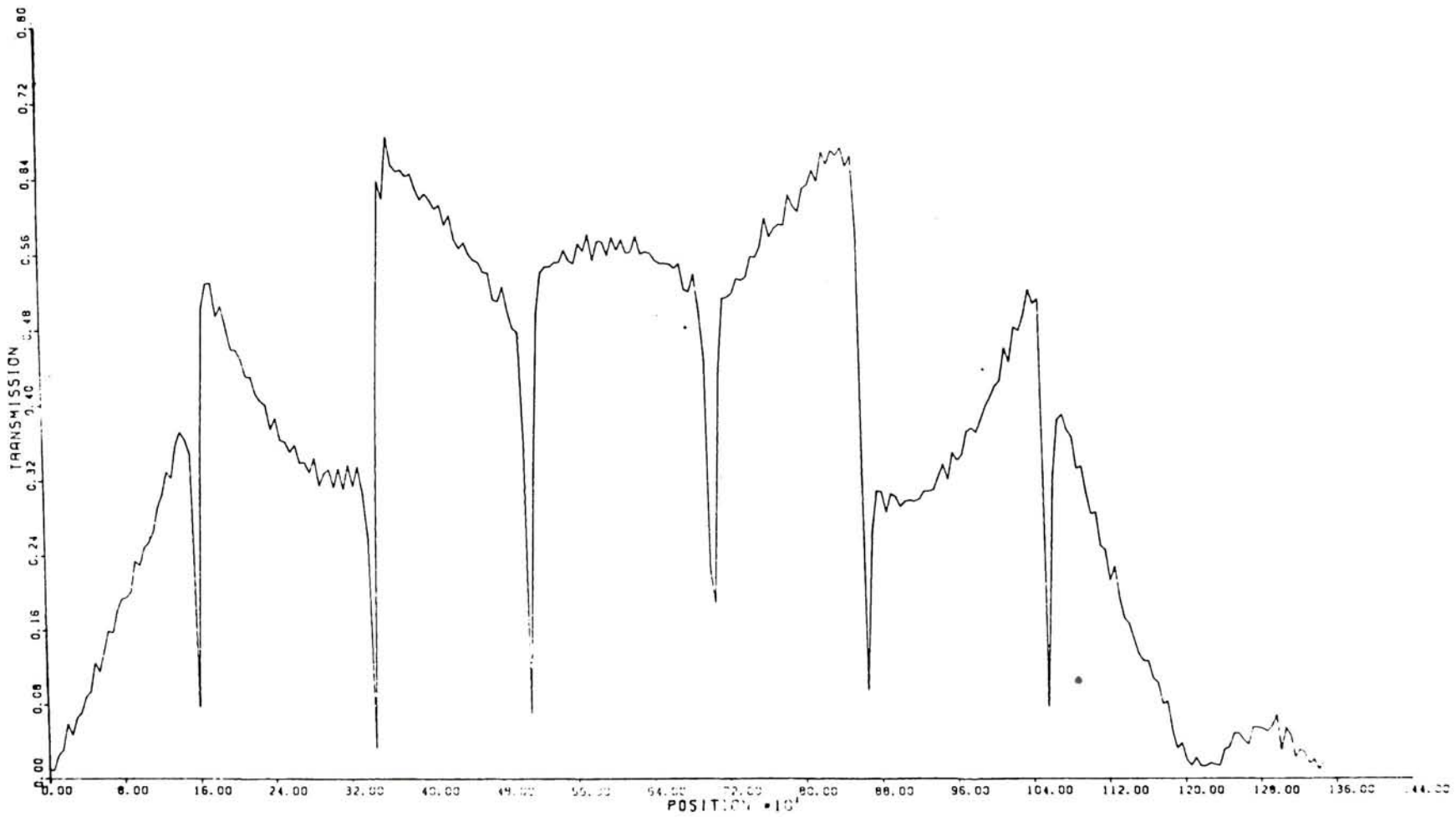

BARTARGET- Ideal High Pass Filter, f_c= 2 cycles/mm

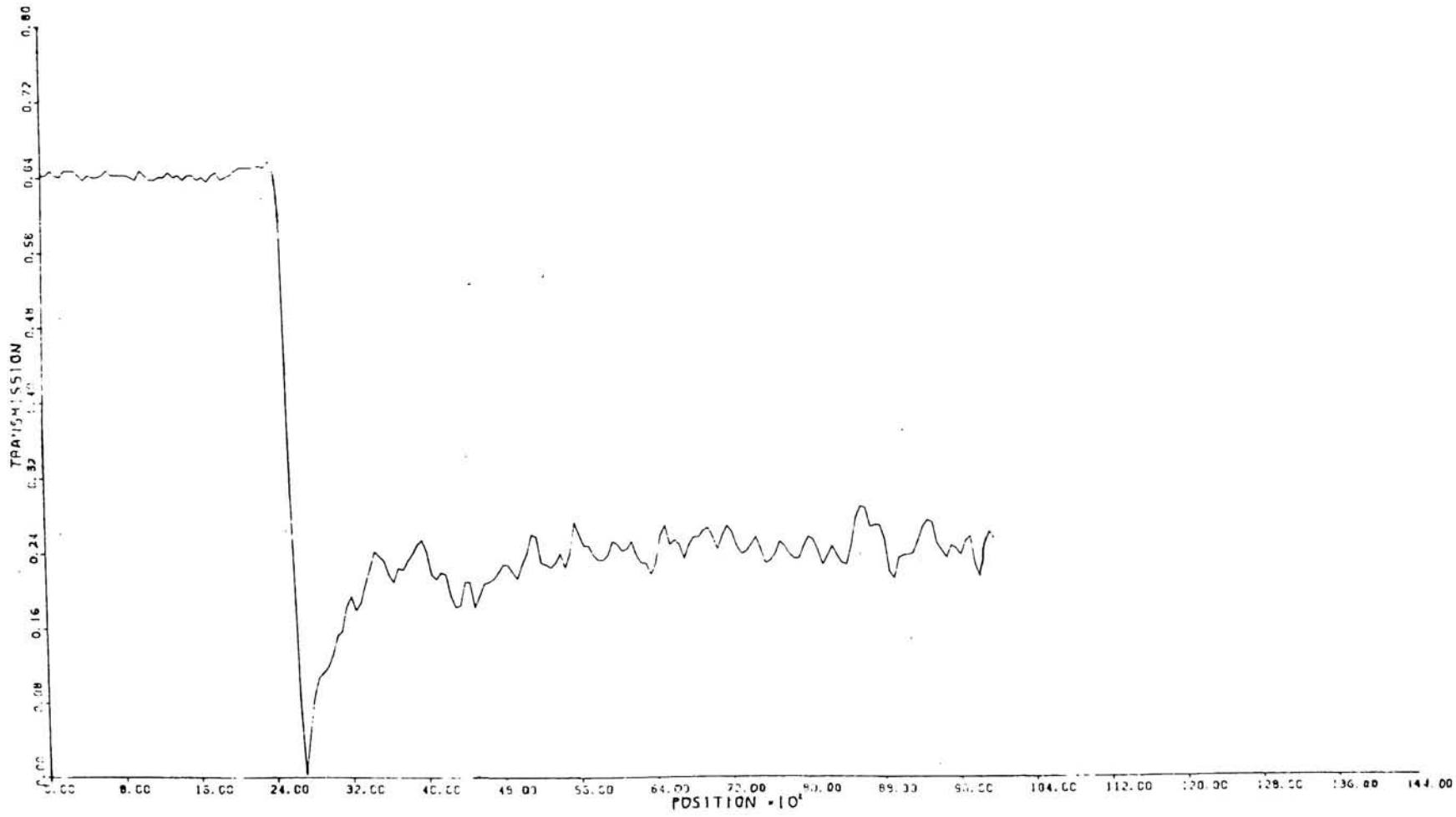

EDGE- Ideal High Pass Filter, f_c= 1 cycle/mm

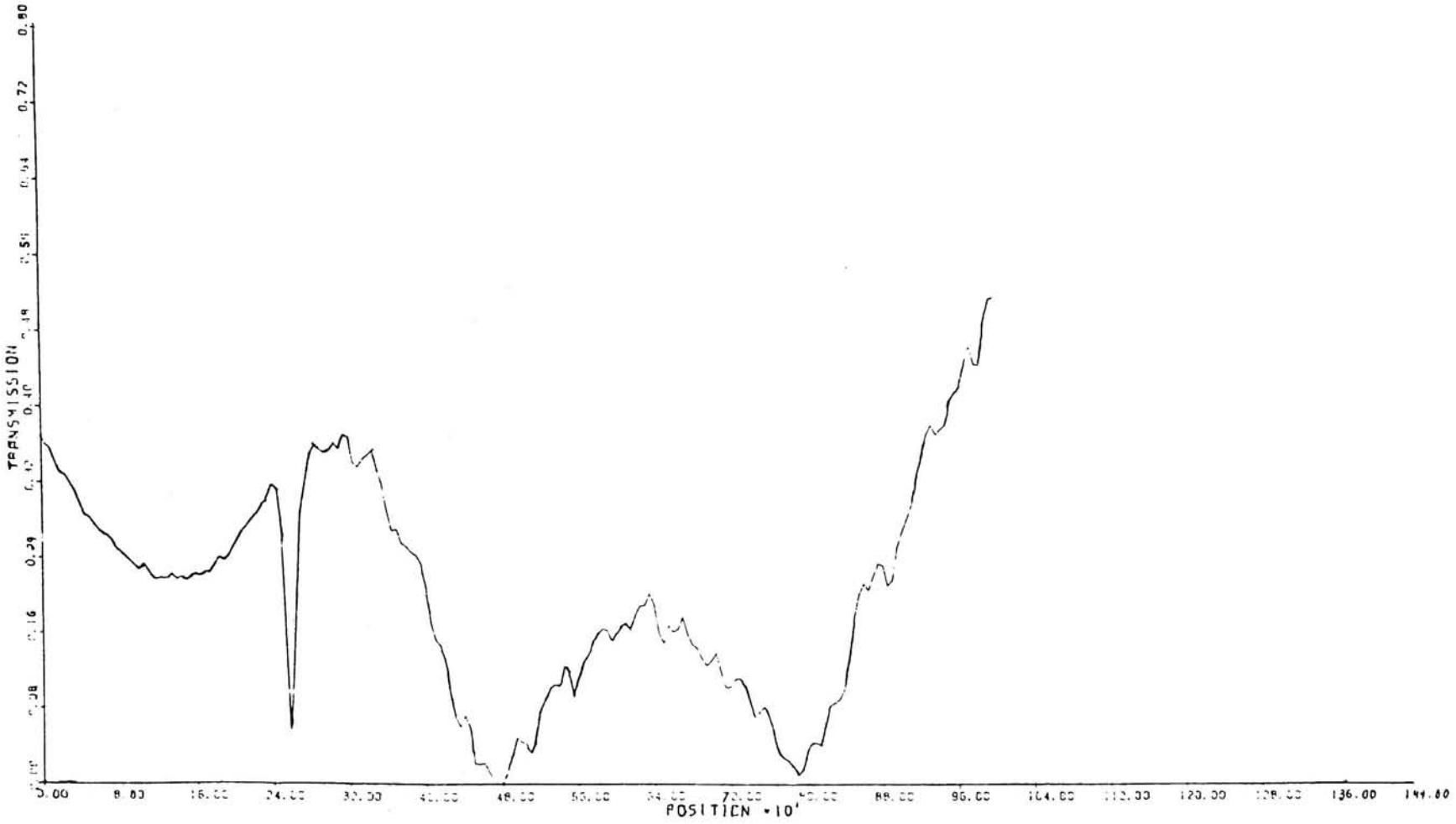

EDGE- Ideal High Pass Filter, f_c= 2 cycles/mm

follows from what was determined earlier, that the noise is contained at the high frequencies of the transform. Since the magnitude of the high frequencies is unaffected by the IHPF, the absolute magnitude of the noise will remain constant, while the level of the signal is reduced. The reason for the increase in transmissions of the originally low transmission areas is not fully understood, but may be a result of the fact that the IHPF produces a large discontinuity in the Fourier transform of the original image. The filtered transform is a step function which tails off with the values of the original transform after the cutoff frequency. The reconstructed images are therefore the result of the Fourier transform of a step and the remaining part of the original transform. It is this discontinuity in the filtered transform which may result in the strange effect on the areas of low transmission.

The effects of the ELPF parallel those achieved using the ILPF except with one major difference. At a cutoff frequency of 30 cycles/mm the ELPF destroyed or removed all noise from the images. Sharp corners became rounded and the edges lost some sharpness, but not much. Since the level of the signal remains the same and the noise is all but destroyed, the signal to noise ratio is greatly increased by the ELPF. As the cutoff frequency of the filter is reduced, the images become smoother and the less sharp the edges become. At a cutoff frequency of about 5-10 cycles/mm the images were

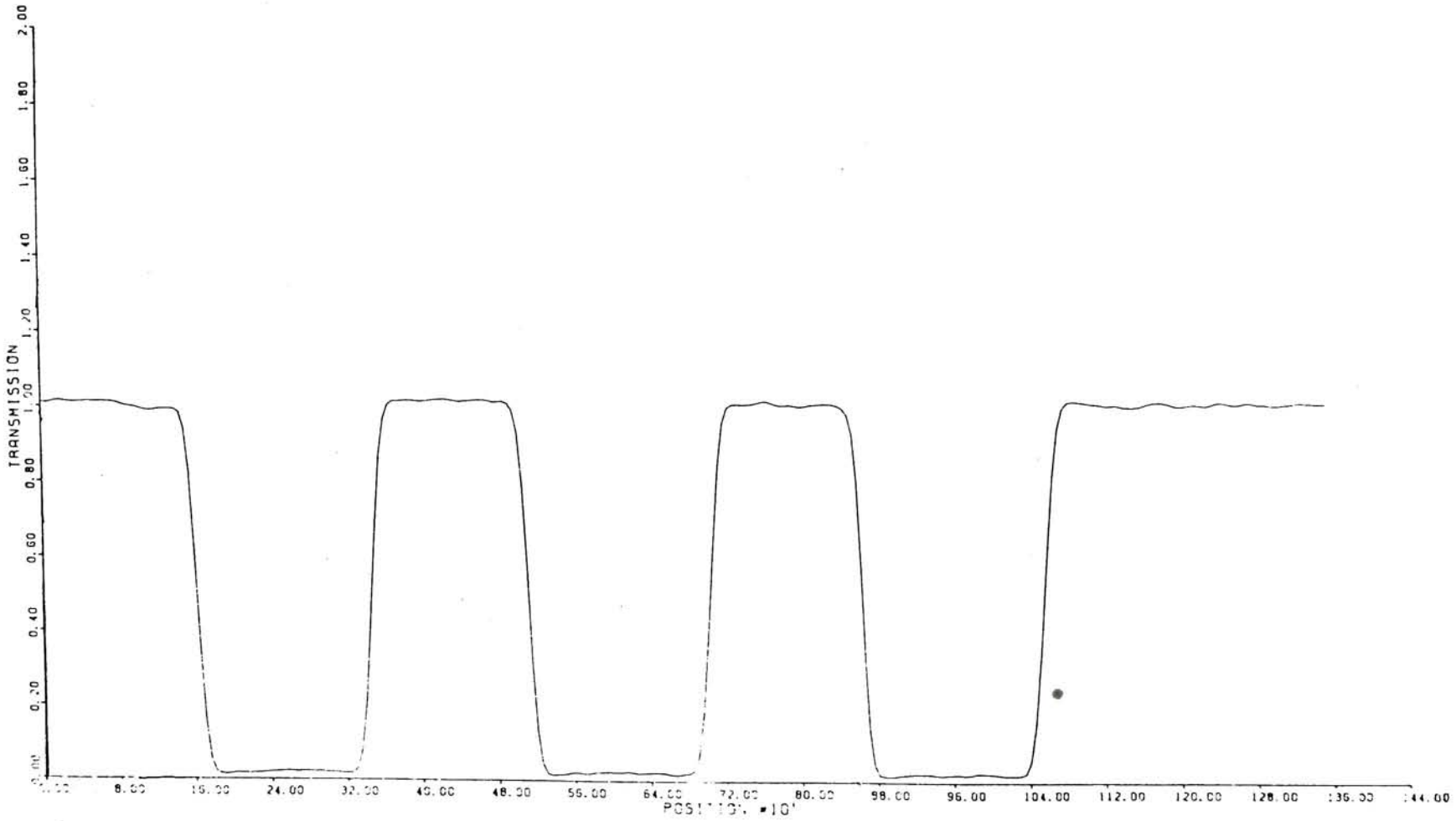

BARTARGET- Exponential Low Pass Filter, f_c= 20 cycles/mm

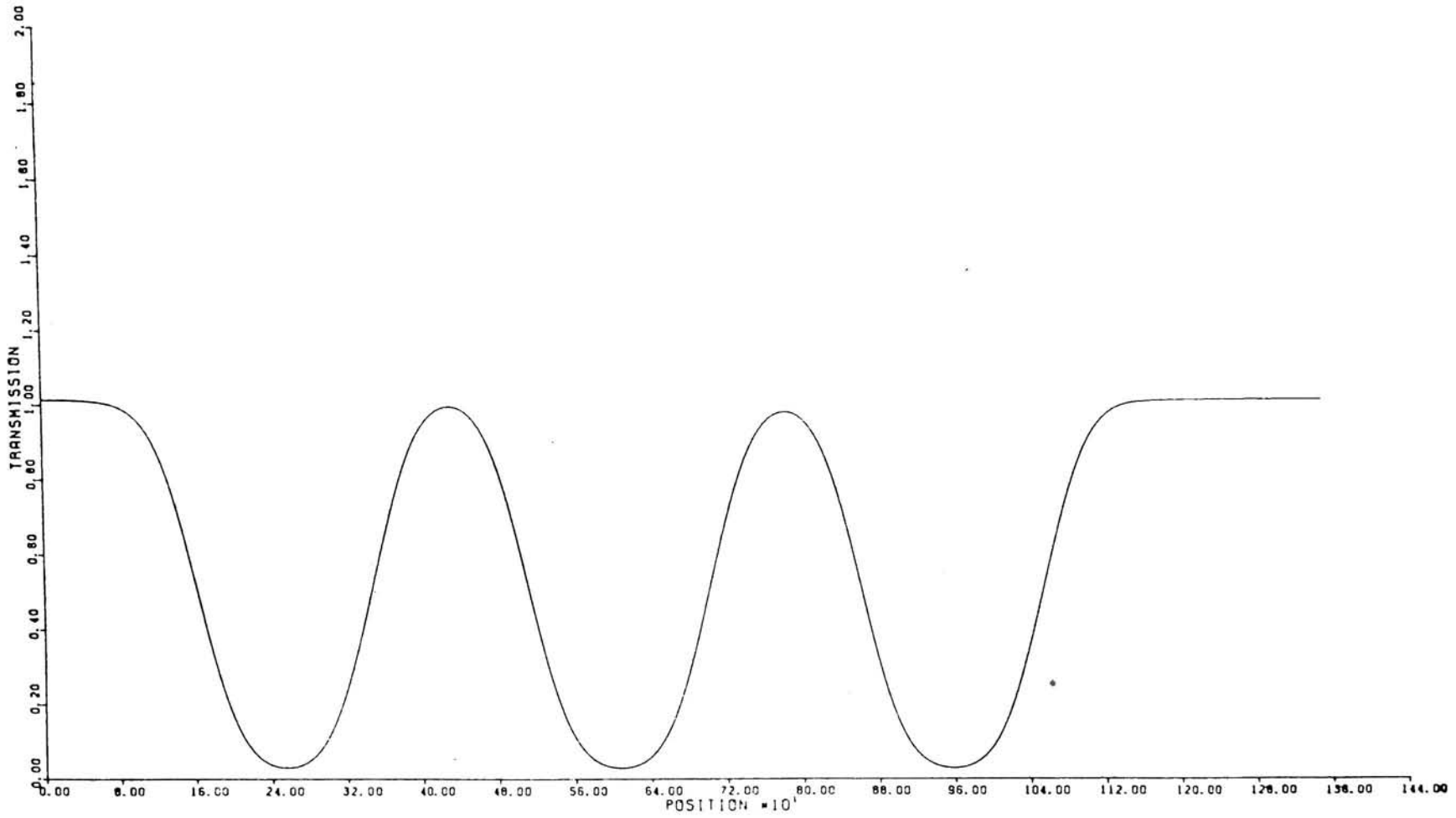

BARTARGET- Exponential Low Pass Filter, f_c= 4 cycles/mm

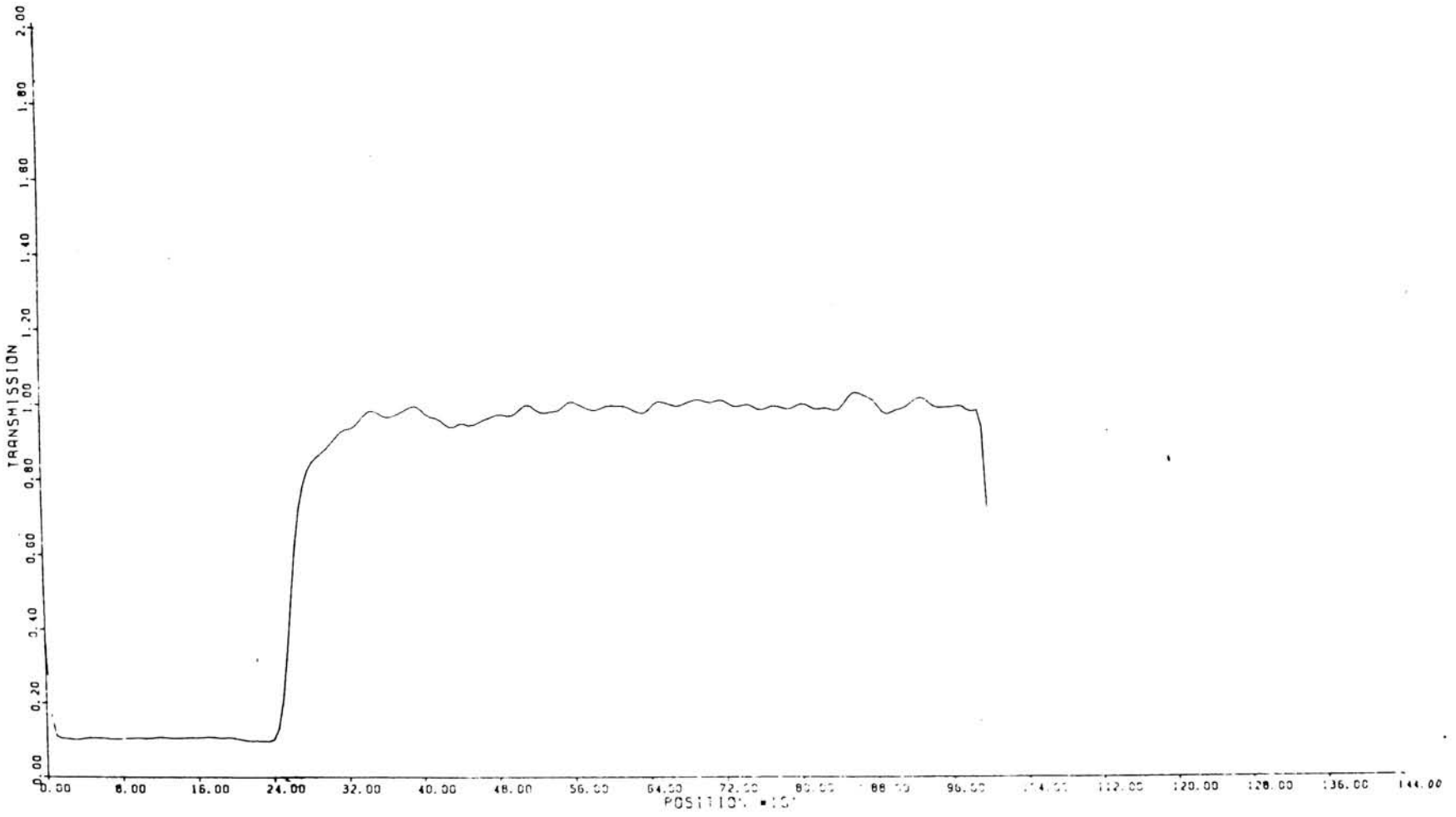

EDGE- Exponential Low Pass Filter, f_c= 25 cycles/mm

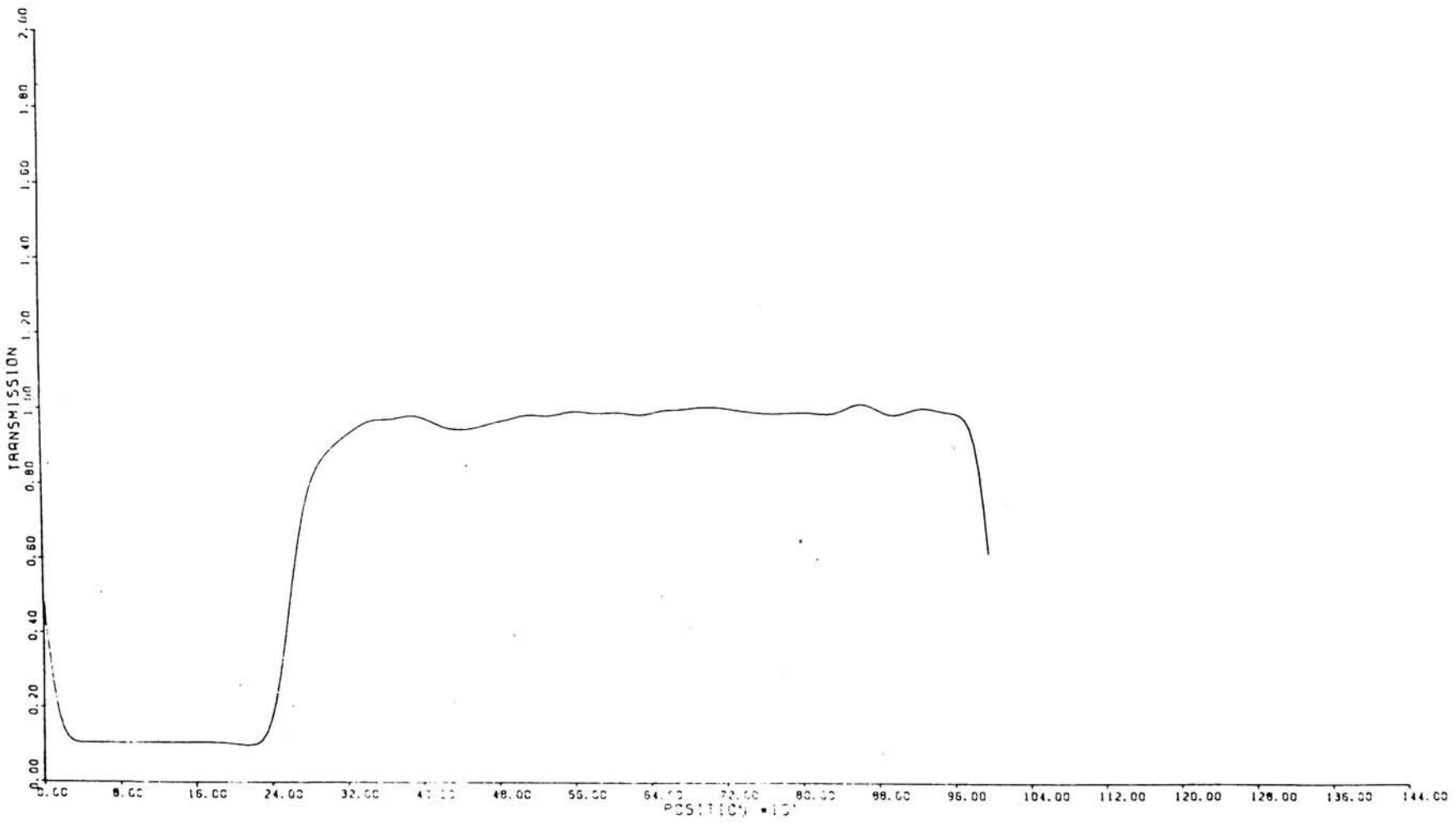

EDGE- Exponential Low Pass Filter, f_c= 10 cycles/mm

very degraded and represented sinusoids more than the original images. One effect that the ELPF had on the edge that it did not correspondingly have on the bartarget, was to produce large error at the end points of the image. As f_c decreased, the error in the endpoints of the edge increased. The most important difference between the effects of the ILPF and the ELPF is that results from the use of the ELPF do not contain "ringing". The form of the ELPF used is Gaussian and the Fourier transform of a Gaussian function is another Gaussian function. The Gaussian function is a very smooth continuous function and so its convolution with the image upon filtering produces a very smooth image. As the cutoff frequency is decreased the width of the Fourier transform of the filter increases, producing a wider Gaussian function in the spatial domain, which is why the images become much smoother as f_c is decreased.

The EHPF did not have the destroying effect that the IHPF had on the images. At a cutoff frequency of 80 cycles/mm both images are composed primarily of noise. At f_c= 60 cycles/mm the images are very noisy but both the edge and the bartarget are easily distinguished. As with the IHPF, the EHPF reduced the level of the signal in the images. The lowered level of the signal produced by the EHPF causes the signal to noise ratio to decrease substantially from the original images. As the cutoff frequency used is reduced,

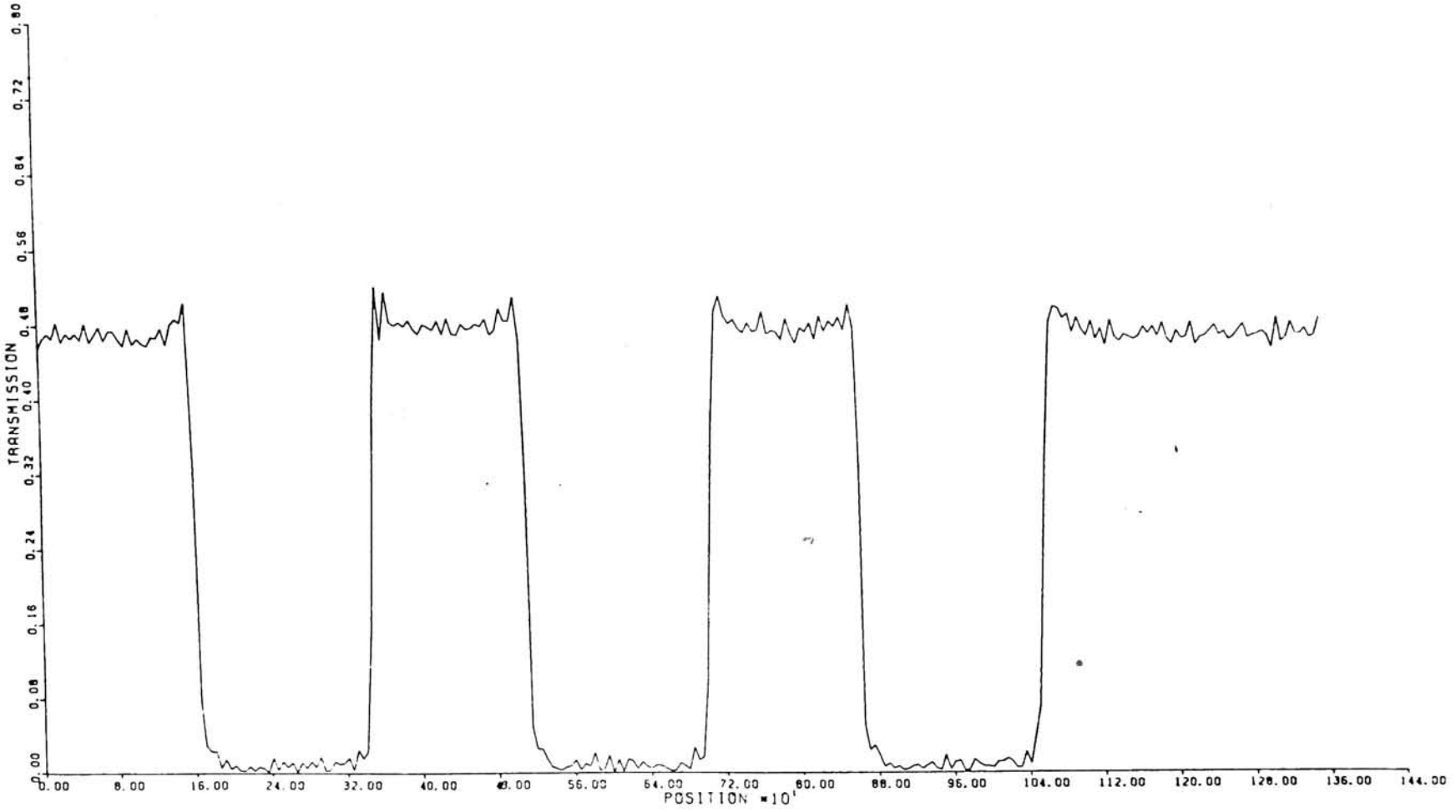

BARTARGET- Exponential High Pass Filter, f_c= 30 cycles/mm

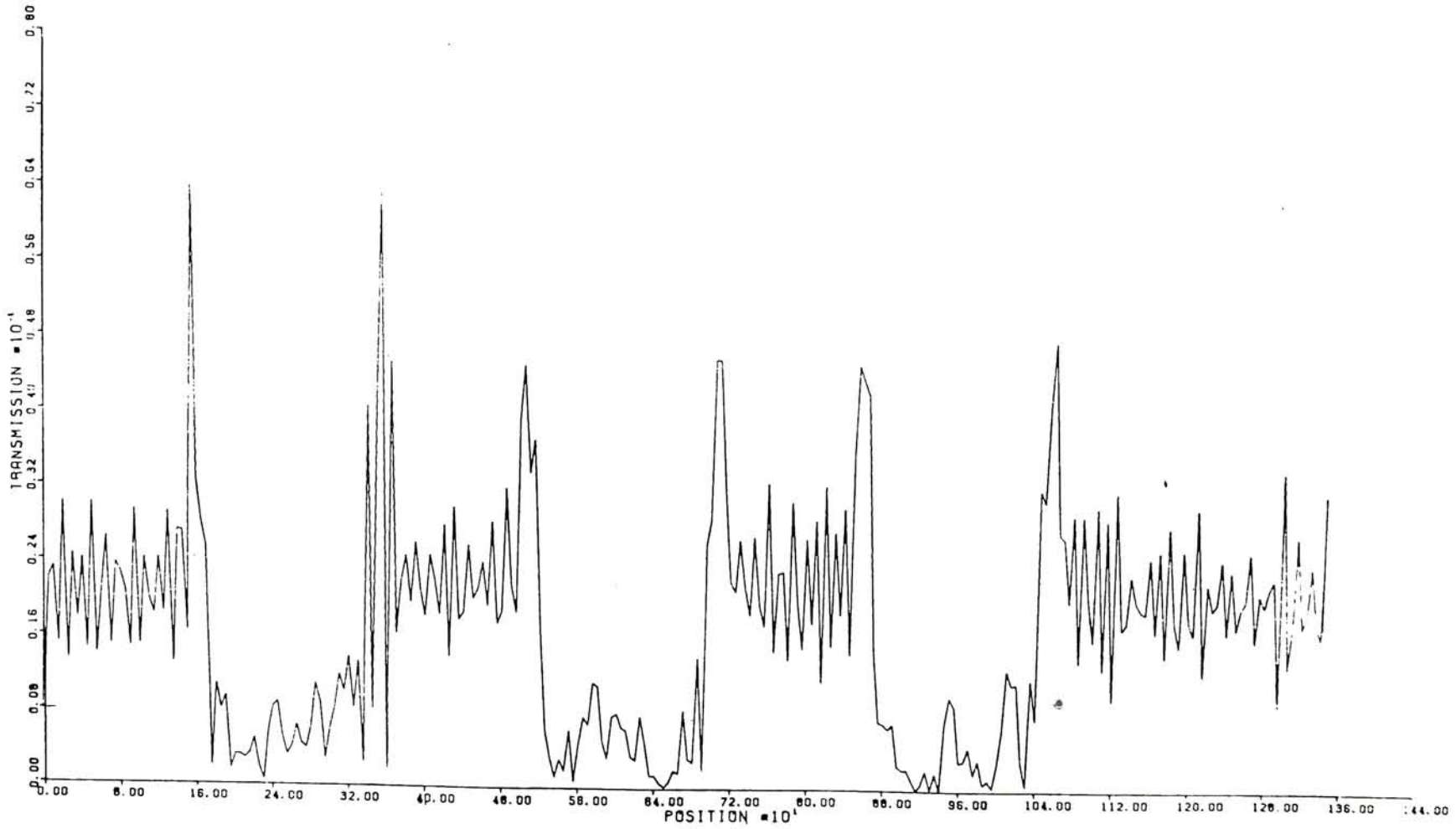

BARTARGET- Exponential High Pass Filter, f_c= 70 cycles/mm

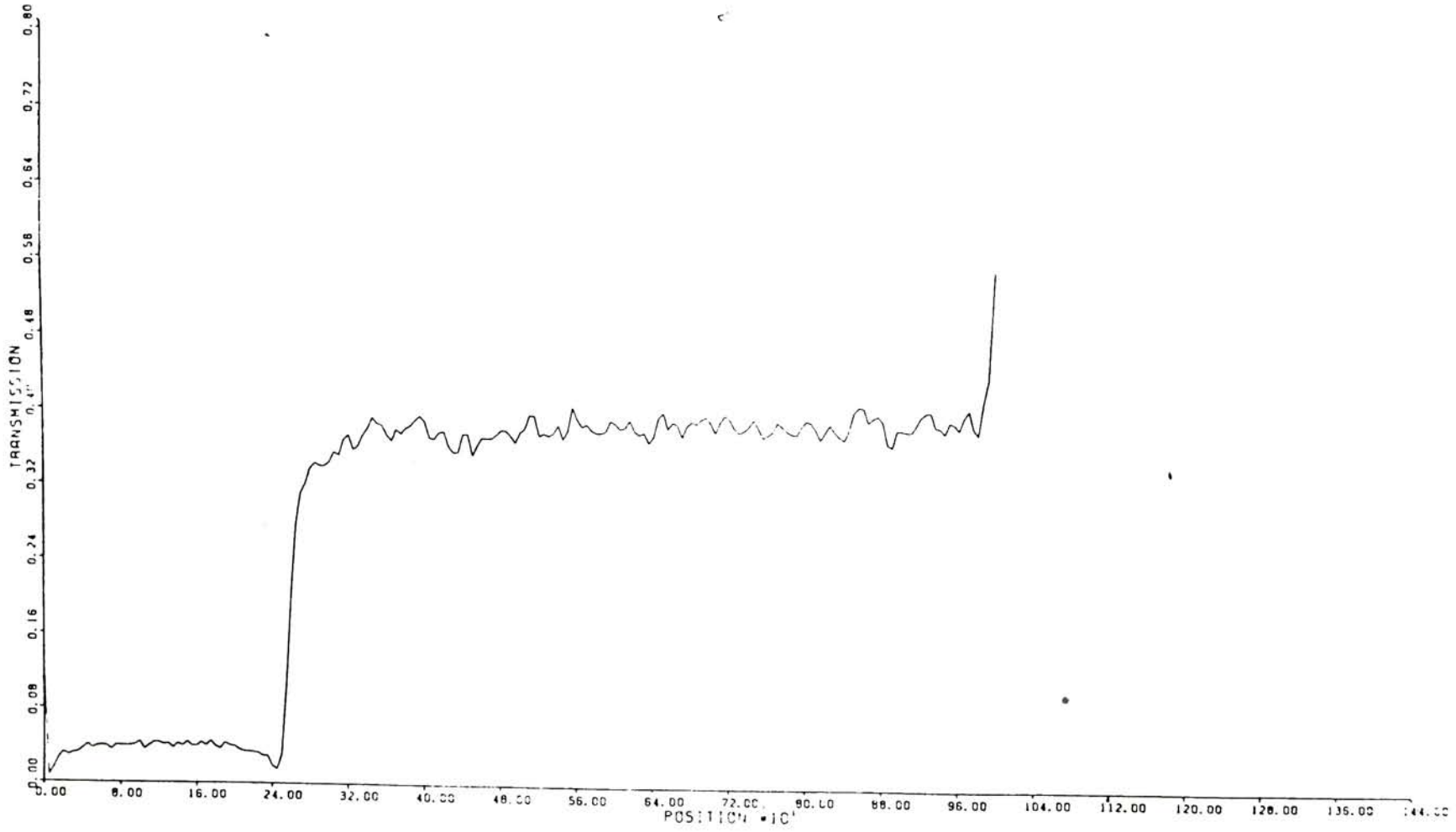

EDGE- Exponential High Pass Filter, f_c= 30 cycles/mm

the level of the signal is also reduced thereby producing a lower signal to noise ratio. An interesting effect encountered when applying the EHPF is that of overshoot at the edges. Overshoot is a condition where the transmission of the image at a point on or near a major transition is much higher than the level of the signal should be compared to the surrounding region. This is known as the Gibb's phenomenon. This condition of overshoot is in opposition to the conditions previously mentioned, that is, the reduction of the signal to noise ratio. The condition of overshoot causes the image to appear to be sharper because the change in the level of the signal occurs over a larger range of transmission. However the reduced signal to noise ratio causes the detection of a signal from the background to become more difficult.

The high frequency emphasis exponential high pass filter had very little effect on the images until a cutoff frequency of about 20 cycles/mm was reached. At low cutoff frequencies the high frequency emphasis filter caused the level of the signal to increase, but did not affect the image in any other way. The quality of the edges and the magnitude of the noise were unaffected by the filter. Little or no effect on the sharpness of the edges and the magnitude of the noise was produced because of the fact that the magnitude of the Fourier transforms at high frequencies is so small. Even

where the amplitude of the higher frequencies was increased by a factor of two, the change relative to the amplitude of the lower frequencies is negligible. Only when the filter starts to affect the relative amplitude of the lower frequencies did a change occur in the images. The transmission range of the image is increased as would be expected since the amplitude of those frequencies from which the structure of the image is based is being increased.

The effect of aliasing could not be graphically demonstrated because the changes produced were small in comparison to the maximum magnitude of the transforms. Both transforms fell to very small values at relatively low frequencies and so even large changes were very small in comparison to the magnitude of the transform at very low frequencies. However when the amplitude of the transforms of the differently sampled images were compared frequency for frequency, differences became more apparent. A significant increase in the amplitude of the Fourier transform of the image sampled at 10μm intervals was detected at about 30 cycles/mm. The increase being in the range of 10-20%. For sampling done at 15μm intervals a significant difference was detected at 20 cycles/mm. Increases again fell in the 10-20% range. Aliasing did not become significant until about 15 cycles/mm for a sampling interval of 20μm. Actual locations where aliasing becomes significant were hard to

pinpoint because of noise in the tranform. No change in the transform would appear at a relative maximum but then an adjacent sample would demonstrate a significant change in value due to aliasing and then the sample adjacent to that point would be unchanged. In any case, the effect of aliasing in this work was small due to the fact that so little significant information was contained in the transforms past 30 cycles/mm. Any increase in the amplitude of the higher frequencies was insignificant relative to the amplitude of the lower frequencies.

CONCLUSIONS

The relative magnitude of the Fourier transform of an image at various frequencies determines their importance in the construction of the image. Various regions of the Fourier transform control or affect different properties of the image. The amplitude of the low frequencies controls the level of the signal and the shape or form of the image. The amplitude of the high frequencies controls the sharp transitions in the image but not their relative size. Most noise is contained in the high frequency region of the Fourier transform. Removal or attenuation of the lower frequencies in the Fourier transform of the image causes the average level of the signal to decrease, affects the general shape of the image, and lowers the signal to noise ratio. Removal or attenuation of the high frequencies causes the image to become smoother and the signal to noise ratio to increase.

Filters must be designed to fit the specific needs of a given problem. There is no one ideal filter for every situation. There are always tradeoffs which must be considered before a filter can be applied to a problem. A low pass filter will reduce the noise in an image but at

CONCLUSIONS, continued

the expense of fine detail and sharp edges. A high pass filter will cause the image to appear sharper but at the expense of a lower signal to noise ratio. Therefore the perfect filter does not exist, but filters can be designed so that the desired results are optimized before other factors begin to enter into the problem. A knowledge of the image and its Fourier transform is vital in the proper design of filters so that unwanted results are not obtained and that time and energy are not wasted on hit or miss attempts at the solution of the problem.

ACKNOWLEDGMENTS

I would like to express my gratitude towards Professor Mohamed Abouelata and Mr. Jim J. Jakubowski whose guidance made this work possible.

REFERENCES

[1]Ronald N. Bracewell, The Fourier Transform and Its Applications (New York: McGraw-Hill, 1978), p. 356.

[2]Ibid.

[3]Oran E. Brigham, The Fast Fourier Transform (Englewood Cliffs, New Jersey: Prentice-Hall, Inc., 1974), p. 93.

[4]Rafael C. Gonzalez and Paul Wintz, Digital Image Processing (Reading, Massachusetts: Addison-Wesley, 1977), p. 70.

[5]Brigham, The Fast Fourier Transform, p. 94.

[6]Ibid., p. 96.

[7]Ibid., p. 93.

[8]Ibid., p. 96.

[9]Jack D. Gaskill, Linear Systems, Fourier Transforms, and Optics (New York: John Wiley and Sons, 1978), pp. 112-113.

[10]Brigham, The Fast Fourier Transform, p. 97.

[11]Ibid., p. 98.

[12]Gonzalez and Wintz, Digital Image Processing, p. 70.

[13]Brigham, The Fast Fourier Transform, p. 85.

[14]Gonzalez and Wintz, Digital Image Processing, p. 70.

[15]Brigham, The Fast Fourier Transform, p. 96.

[16]Ibid., p. 134.

[17]Ibid.

[18]Ibid., p. 149.

[19]Ibid., p. 18.

REFERENCES, continued

[20]Gonzalez and Wintz, Digital Image Processing, p. 79.

[21]Ibid., p. 199.

[22]Jim Jakubowski, Xerox Corporation, personal communication.

[23]Professor John F. Carson, Rochester Institute of Technology, personal communication.

[24]Jim Jakubowski, personal communication.

[25]Gonzalez and Wintz, Digital Image Processing, p. 141.

[26]Ibid., p. 162.

[27]Ibid., p. 148.

[28]Ibid., p. 166.

[29]Gaskill, Linear Systems, Fourier Transforms and Optics, p. 110.

BIBLIOGRAPHY

Bracewell, Ronald N. The Fourier Transform and Its Applications. New York: McGraw-Hill, 1978.

Brigham, E. Oran. The Fast Fourier Transform. Englewood Cliffs, New Jersey: Prentice-Hall, Inc., 1974.

Gaskill, Jack D. Linear Systems, Fourier Transforms, and Optics. New York: John Wiley and Sons, 1978.

Gonzalez, Rafael C. and Paul Wintz. Digital Image Processing. Reading, Massachusetts: Addison-Wesley, 1977.